

Results of Detailed Synoptic Studies of Squall Lines

By TETSUYA FUJITA, Kyushu Institute of Technology and University of Chicago¹

(Manuscript received June 15, 1955)

Abstract

A system of synoptic analysis on a mesometeorological scale has been developed through the combined use of space and time sections applied to all regular and special stations in an area 500 by 900 mi. in the Central United States. Two periods of development of large thunderstorm areas are analyzed. In both of these periods tornadoes occurred. The synoptic model of a squall line in this scale involves three principal features of the pressure field—the pressure surge, the thunderstorm high and the wake depression. Another feature, called the tornado cyclone, accompanies tornado funnels. Divergence values of 10 to $60 \cdot 10^{-5} \text{ sec}^{-1}$ over areas of 100 to 10,000 sq. mi. are measured. The mesosynoptic disturbances greatly influence the situation as viewed on the regular synoptic scale, which is about 10 times the meso-scale, and make conventional analysis hopelessly difficult.

1. Introduction

Severe storms such as thunderstorms, hail, high wind, and tornadoes usually occur in close relation to disturbances with linear dimensions of 10 to 100 miles. The analysis dealing with this scale is termed mesoanalysis. The term "mesometeorology" has been used in studies of radar meteorology by SWINGLE (1953) and others. The analysis of systems with dimensions of 100 to 1 000 miles or more is involved in the usual daily synoptic practice.

Studies of micro-scale disturbances, smaller than 10 miles, are typified by the Thunderstorm Project (BYERS, BRAHAM, 1949) in Florida (1946) and Ohio (1947). Microanalysis was carried out for weather elements such as pressure, temperature, radar echo, wind direction and speed, divergence, etc. The five-minute interval chart sequences revealed the microstructure of the thunderstorm circulation.

Using the data from the automatic recording

stations in Ohio operated by the U.S. Weather Bureau's Cloud Physics Project in 1948, WILLIAMS (1948) studied the microstructure of the squall-lines. In this chart the microstructure of the pressure and temperature systems is well represented by the five-minute interval analysis. TEPPER (1950) studied the microstructure of the "pressure jump" line traversing the area of the 1948 Ohio network. The one-minute interval charts he made show the isallobars for the amount of the pressure increase following the "jump". His study made it clear that there exists a very tight pressure gradient in a narrow zone where the winds are very far from being geostrophic. The micro-analysis of the thunderstorm high of Aug. 24, 1947, over Kyushu, Japan was done by the writer (FUJITA, 1950) on the basis of ten-minute interval charts for an area of 60 by 50 miles. The chart sequence shows that the thunderstorm high, having a very tight pressure gradient, deforms when it passes over mountains.

Other earlier microscale or mesoscale analyses include the well-known Norwegian charts published in the early 1920's leading to the

¹ The research reported in this paper has been sponsored by the Geophysics Research Directorate of the Air Force Cambridge Research Center, Air Research and Development Command, under contract AF 19(604)-618.

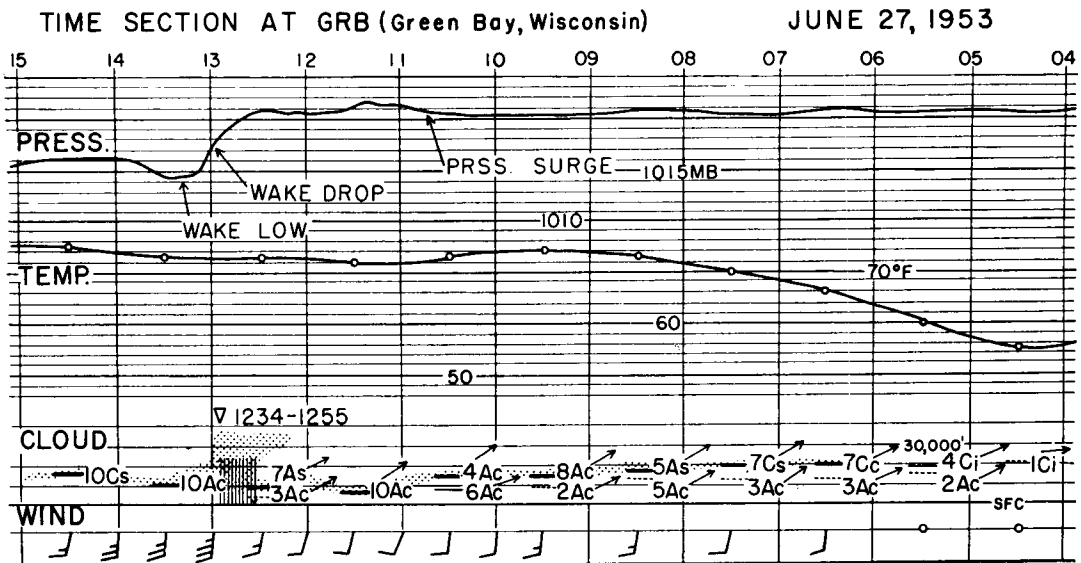


Fig. 1. Example of time section.

discovery of air-mass and frontal analysis, the micro-studies of SUCKSTORFF (1953) in connection with thunderstorms, the charts of the U.S. Soil Conservation Service in the Muskingum Valley, used by BYERS (1942), and studies by C. F. BROOKS (1922). The author asks forgiveness for failing to mention others.

The cold front of September 26—27, 1948 was also analyzed by the writer (FUJITA, 1951). From the pressure, temperature, wind and rain traces of stations in Western Japan, the 20-minute interval charts for pressure, temperature, and rain were constructed. The area covered by the study was 300 by 200 miles. In that area, the stations were scattered, the average separation being 60 miles. This was an early stage of meso-analysis.

BERGERON (1954) made analyses of a pseudo-cold-front over the Middle West, and emphasized the importance of the cooling effect of rain, in order to explain the divergence field beneath squall-line thunderstorms.

In the studies carried out by the writer at the University of Chicago under the general guidance of Dr Horace R. Byers, many important features of the meso-scale disturbances became clear. Most of the tight pressure gradients associated with squall line activity, which Tepper calls "pressure jumps", are now known to be the result of the huge thunder-

storm high produced by squall-line thunderstorms. To distinguish the pressure rise at the front of the thunderstorm high from the hydraulic jump, which demands adherence to an analogy from hydraulics, Dr Byers and the writer chose to call it "the pressure surge."¹ Following the surge, "the thunderstorm high" comes, then the pressure falls gradually or very rapidly. This fall is due to effects in the wake of the thunderstorm high which usually moves rapidly with the direction of the wind aloft. The low pressure areas following the "wake depression" in pressure we will designate as the "wake depression." These features are illustrated in Plate 4.

2. The time and space section

The average separation of the teletype stations in the Middle West of the United States is about 100 miles. If one plots the data in the usual way employed on daily synoptic charts,

¹ Definition of "surge" in the *Meteorological Glossary*: First used by Abercromby to denote a general change of pressure superposed upon the changes which are due to the movement of DEPRESSIONS and ANTICYCLONES.

In the *Weather Glossary*, U.S. Dept. of Commerce, Weather Bureau, it is said that "surge means any change of pressure over a wide area, the precise cause of which is unknown, but which is not due to the passage of low or high pressure areas or to diurnal barometric variation".

using the hourly reports from these stations, it would be very difficult to analyze the meso-scale disturbances.

The time section of the weather elements from each station will give added information about the weather conditions in the areas between stations. An example of the time section is shown in Fig. 1. As will be seen in the figure, the time runs from right to left, so that in the zone of the westerlies the time section becomes very similar to the space section running through the station in question. In the time section, we must enter all available observations. To this end, the original data used in this study include:

- (1) Hourly Teletype Sequences. Report of the amount and the height of the cloud base, sea-level pressure, temperature and dew point, wind, remarks, etc. The time of observation is about 28 minutes after the hour.
- (2) Special Weather Report on Teletype. Report of the events occurring between the regular hourly observations. Usually, pressure and temperature do not appear. In the 1130 Form kept in the National Weather Record Center, Asheville, all of the hourly and the special observations not sent out by teletype are shown.
- (3) Self-recorded Traces. Pressure, temperature, humidity, wind, and precipitation traces kept in the National Weather Records Center.
- (4) Traces from the Severe Storm Research Unit in the U.S. Weather Bureau. About 200 accelerated barograph, 30 hygromograph and some wind and precipitation from stations maintained in the Middle West. The traces from these stations are excellent material for the meso-analysis.
- (5) Hourly precipitation data and Climatological Data. These are published by the U.S. Weather Bureau. In the Hourly Precipitation Data, the hourly amounts of the rain from stations all over the United States are tabulated. Average separation of the stations is 30 to 40 miles. The daily amount of precipitation measured either in the a.m. hour or the p.m. hour is shown in the Climatological Data. Average distance of the stations is 10 to 20 miles.

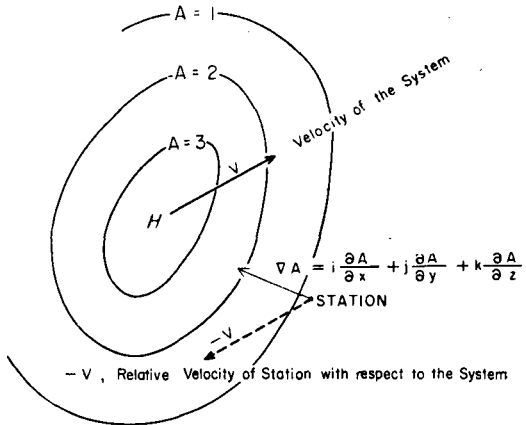


Fig. 2. Relative velocity of a station with respect to a moving system.

Making use of these data, one must construct the time section for each station before the meso-analysis is carried out. As will be seen in Fig. 1, pressure, temperature, height and amount of cloud, movement and type of cloud, and wind speed are plotted carefully. After making the time section, it is better to indicate the significant points such as pressure surge, wake drop, wake low, temperature break, etc.

Time sections made for each station can be changed into a space section on the synoptic chart. As shown in Fig. 2, the relative velocity of a station with respect to a moving system is $-V$. It is convenient to use the conventional relationship used in hydrodynamics for the local and individual change in a moving system. If we regard the station as moving with respect to the system, the individual change of the element A , that is, dA/dt may be considered as the change at the station moving with relative velocity $-V$. Then $\partial A/\partial t$ is the change in the system. The formula is

$$\begin{aligned} dA/dt &= \partial A/\partial t + (-V \cdot \nabla A) \\ &= \partial A/\partial t - V \cdot \nabla A \end{aligned}$$

In the case, where the system does not change rapidly, the formula can be reduced to

$$\frac{dA}{dt} = -V \cdot \text{grad } A$$

From this equation, the time change can be converted into the space change. Practically,

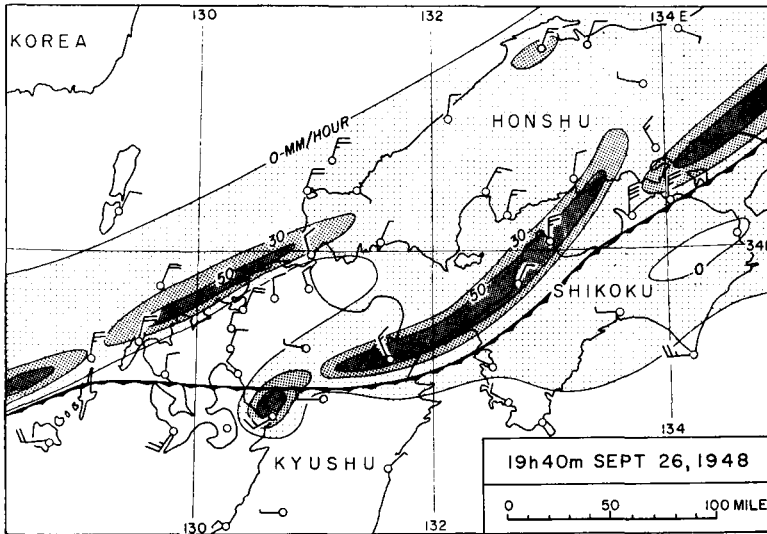


Fig. 3. Rain intensity chart of the cold front at 1940, Sept. 26, 1948 over West Japan.

however, the change of the system is taking place rather quickly. Techniques dealing with this problem will be discussed in the chapter on pressure analysis.

3. Analysis of precipitation

The precipitation traces show the amount of the accumulated rain. In the meso-analysis, we are interested in the distribution of the rain intensity. The traces must be differentiated with respect to time. The rain-intensity curve obtained by the careful differentiation are entered in the time section charts. An example of the rain intensity charts for the squall-line over West Japan in 1948 is shown in Fig. 3. To draw the isohyets, the traces from the 60 stations in the areas are used. The two rain bands are pushing toward the east-south east.

The available precipitation traces in the Middle West are not sufficient in number to permit construction of the rain intensity pattern. Isohyets for the hourly precipitation amount can be drawn in this case.

Before making the hourly precipitation charts, it is useful to draw the isohyets for the total amount of the rainfall accompanying the storm under study. The total precipitation chart shows the areas where the heavy rain showers have passed and thus gives an important clue to the areal distributions.

Percentage Method

A percentage method is used in which the precipitation reported by the daily observation station can be converted into the total rainfall amount for a particular storm. Consider the hourly rain from the hourly observation stations in Fig. 4. R_1, R_2, \dots are the rain accompanied by the storm B in which we are interested. If these were the daily observation stations, they would report the rainfall amounts R'_1, R'_2, \dots on the 23rd, for instance. The amount of R is not always equal to that of R' , since the period is different. Taking the ratios

$$\frac{R_1}{R'_1} = r_1, \quad \frac{R_2}{R'_2} = r_2, \quad \frac{R_3}{R'_3} = r_3 \dots$$

for each hourly observation station, we plot them on the map. An example will be seen in Fig. 5, in which the values of r computed by the formula,

$$r = \frac{R}{R'_{27+28}} = \frac{\text{amount of rain accompanying storm of 26-28 June, 1953}}{\text{sum of daily amounts measured at 6 p.m. on 27 and 28 June, 1953}}$$

The iso-percentage lines in the figure show that the ratios are 1.00 (charted as 100) in most of the areas. The sum of the daily precipitation

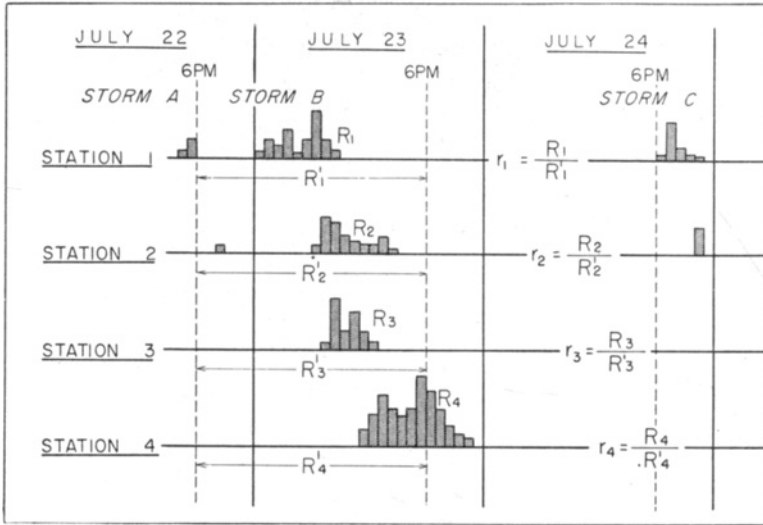


Fig. 4. Example of rainfall plot for applying the "percentage method".

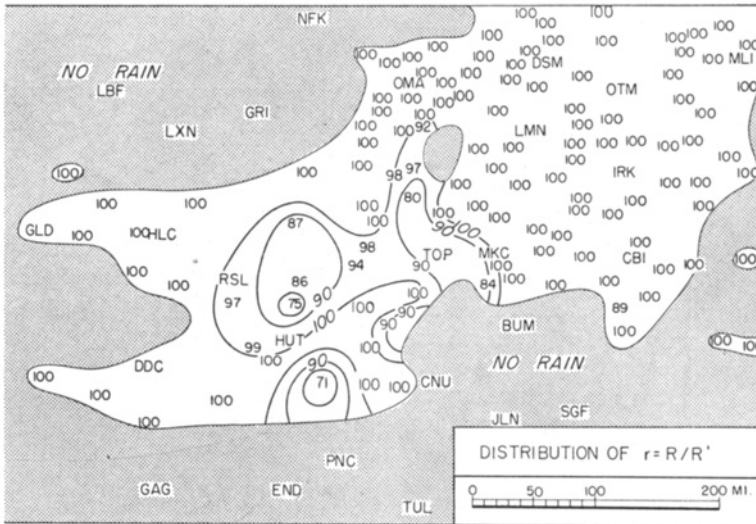


Fig. 5. Distribution of the ratio $r = R/R'$ for the period of June 27-28, 1953. (Center of map near Kansas City—MKC.)

amounts on 27th and 28th June, 1953 can in such circumstances be used as the total amount of rain brought by the storm of 26-28 June. In the other areas where the ratios are not equal to 100, we plot the location of the daily observation station on the iso-percent chart and read the value of r for each station. Let r_0 be the ratio for the daily observation station where the daily rainfall of R'_0 was observed. R_0 , the rain-

fall accompanied by the particular storm, can be computed by the relation,

$$R_0 = R'_0 r_0$$

As an example, the total rainfall for the storm of 26-28 June, 1953 is shown in Fig. 6. Isohyets in the chart are contoured for every 0.20 inch. In the map area, we have about 600 hourly observation stations. By using the

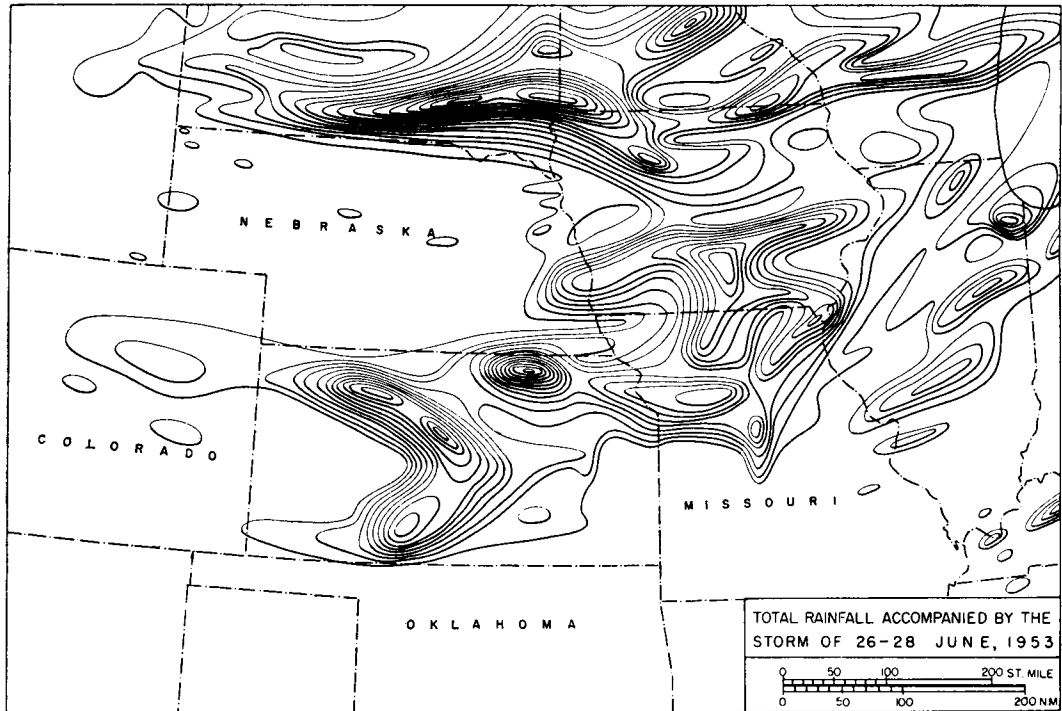


Fig. 6. Total precipitation amount caused by the storm of June 26—28, 1953. The amounts are contoured for every 0.20".

percentage method, 2,400 daily observation stations are used in addition to the hourly observation stations.

The percentage method can be utilized also in obtaining the hourly precipitation amount from the total precipitation. For this purpose, the ratios of the hourly precipitation to the total precipitation are computed for all the hourly observation stations. Then we plot them on the chart, and draw the iso-percentage lines. Superimposing the iso-percentage lines on the isohyet chart made for the total precipitation amount, we make the multiplication of

(total amount of rain) \times (percentage of hourly rainfall / total rainfall). In this process, the total amount of rain is separated into the hourly amount.

4. Analysis of wind

The time section of the observed winds must be converted into the space section in the scale of the wind map. The direction of

the line in the wind chart, along which the winds for each station will be plotted, is that of the movement of the particular system we want to analyze. Usually, the winds for one hour on both sides of the map time are entered on the chart. If several winds are available in the immediate vicinity, the one observed closest to the map time should be used when changing the time section into the space section. From these winds plotted on the chart, the isotachs and the stream lines are drawn.

Divergence and convergence of the wind field are computed next. The computation of the values can be done by using the formula

$$\text{div}_2 = \frac{\Delta u}{\Delta x} + \frac{\Delta v}{\Delta y}$$

The writer developed the method of obtaining convergence from the balance of the net inflow and the outflow.

Method of Computation

Consider the streamlines CA and DB in Fig. 7. The curves AB and CD are the orthogo-

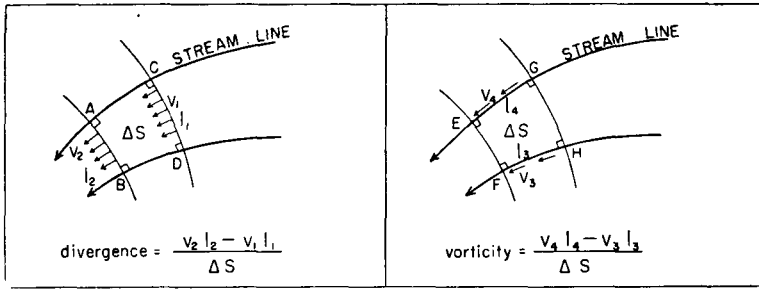


Fig. 7. Method of computation of divergence and vorticity.

nal trajectories to the streamlines with intercepts of length l_1 and l_2 between the streamlines. If the mean speed of the winds passing across CD and AB be v_1 and v_2 respectively, the convergence inside the area ΔS is given by

$$\text{Conv}_2 V = \frac{v_1 l_1 - v_2 l_2}{\Delta S}$$

or

$$\text{Div}_2 V = \frac{v_2 l_2 - v_1 l_1}{\Delta S}$$

As shown in Fig. 7, the vorticity of the wind field can also be computed in a similar way.

Computation Scale

It is possible for us to compute these quantities by using the celluloid computation scale reproduced in Fig. 8. The scale has a straight indicator OQ movable around the eyelet at o. On the celluloid plate, the speed, speed \times length, and the area scales are shown. As will be seen in the figure, the vertical lines with

wind speed at the top and the bottom are so spaced that the distance from the point o is inversely proportional to the wind speed. To the right, the scale of the speed times length ($v \cdot l$) is shown. At the bottom, the various areas are shown by the circles with the numbers showing the values of $l/\Delta S$.

Drawing the streamlines and the orthogonal trajectories, we divide the whole area of meso-analysis into areas (ΔS) like those in Fig. 7. To compute the convergence, we put the celluloid scale, for instance, on Fig. 7, so that the point A comes just under the intersection of the horizontal line OP and the vertical line having the wind speed v_2 . Then we rotate the celluloid plate around A, until B comes right under the line of v_2 . The value of $v_2 l_2$ can be read on the right scale by moving Q downward until OQ passes through the point B. It is evident, from the law of triangles, that the product, windspeed \times length ($v \cdot l$) is obtained on the righthand scale.

An example of the computed result is shown in Fig. 9. This is the micro-analysis of the wind field beneath the thunderstorm in its dissipating stage. The chart in the lower left is made first, and the isotachs shown in the lower right are drawn. Superimposing the streamline chart on the isotach chart, we read the wind speed values in the upper right chart. Finally, the divergence and convergence are obtained by using the celluloid scale.

Examples of the divergence chart for a squall-line system are presented in the color plates 2 and 3.

5. Analysis of temperature

Micro-scale temperature disturbances are usually superimposed upon the meso-scale temperature field. To represent the meso-dis-

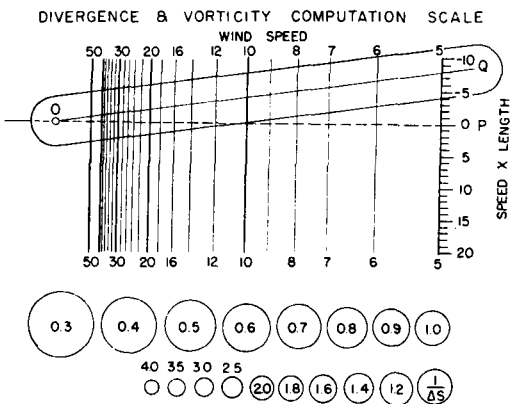


Fig. 8. Computation scale for divergence and vorticity. Tellus VII (1955), 4

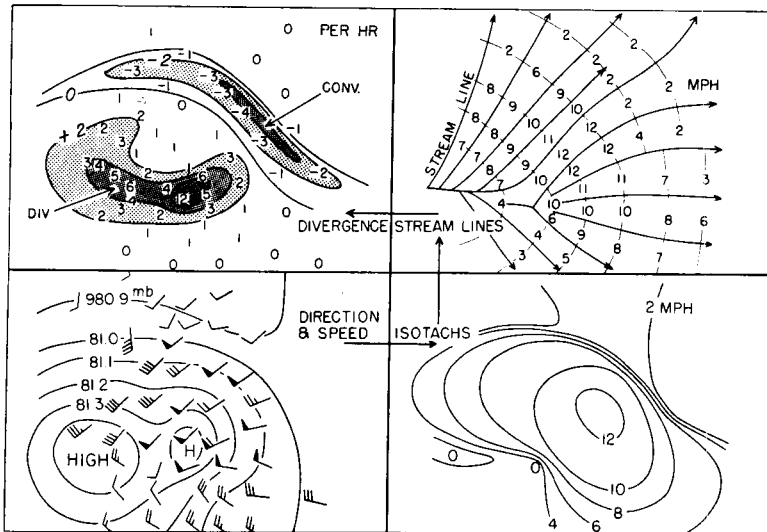


Fig. 9. Example of micro-scale divergence pattern.

turbances effectively, the micro-disturbances, which are caused by the cloudiness, ground condition, vegetation, minor topography or small lakes, shelter exposure problems, etc., must be suppressed.

The isotherms in the upper chart of Fig. 10 are drawn so that they satisfy the plotted values of the mean maximum temperature in June, 1953. One might consider that the drawing of the isotherms is quite adequate, since they are drawn to fit the observed values. This conception is not true. In the middle chart, it is shown that the temperature observed in the small area A, having the same scale as of the upper chart, is different from place to place. Isotherms for the temperature field in question are shown in the same area enlarged. There is no doubt that the isotherms in the upper chart would become just like these which are seen in B, if we could have as many observation stations as in the micro-analysis. The frequency distribution of the observed temperatures in the area A shows the fact that the variation reaches as much as 5 degrees Fahrenheit, as shown on the right of the figure.

The smoothed isotherms shown in the lower chart are the only reasonable ones which can be expected from the data available. The positive and negative values are the amount of correction that must be added to the station temperature, in order to fit the smoothed isotherms.

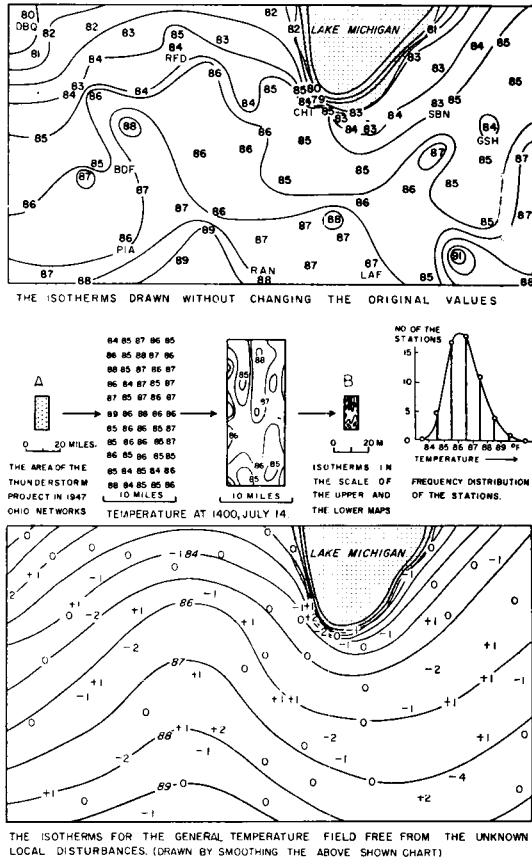


Fig. 10. Application of smoothing method for correction of the mean temperature.

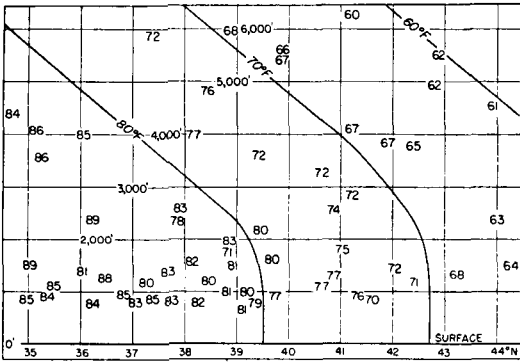


Fig. 11. Chart illustrating reduction of station temperature to sea-level.

Mean Temperature Correction

First, we consider the sea-level correction. The correction will be done by assuming the lapse rate. If we use the lapse rate in the free atmosphere, overcorrection occurs. The writer obtained the lapse rate along the surface for the stations in the Middle West of the United States by plotting the station temperature with respect to the elevation and the latitude. From the inclination of the isotherms drawn in Fig. 11, the lapse rates are known to be 1° F/1000 ft., up to 2000 ft., and 3° F/1000 ft. above 2000 ft.

Let the sea-level temperatures obtained by

the sea-level correction be T, T', T'', \dots etc. They can be written as

$$T = T_0 + T_1 \sin \omega t + \dots T_m \sin m\omega t + \dots$$

$$T' = T'_0 + T'_1 \sin \omega t + \dots T'_m \sin m\omega t + \dots$$

$$T'' = T''_0 + T''_1 \sin \omega t + \dots T''_m \sin m\omega t + \dots$$

where ω is the angular velocity of the earth. In the formulae, T_0, T'_0, T''_0, \dots are the mean sea-level temperature, and T_1, T'_1, T''_1, \dots are the diurnal variations for each station. The meso-scale disturbances having the period of several hours appear in the terms such as $T_{m-1}, T_m, T_{m+1} \dots$ etc. As has been shown in the upper chart of Fig. 10, the isotherms, before they have been smoothed, are very irregular. We can easily imagine that the meso-disturbances analyzed on such an irregular mean temperature field will not show their true features. For the first approximation, the mean temperatures T_0 must be plotted on the chart and then must be corrected by drawing the smooth isotherms.

The smoothed isotherms for T_0 during the period of June 26—28, 1953 are shown in Fig. 12. The mean station temperatures and the amount of correction, smoothed sea-level temperatures minus station temperature are entered on the chart. It will be seen that the amount of correction in the states of Colorado and New Mexico is at most stations more than

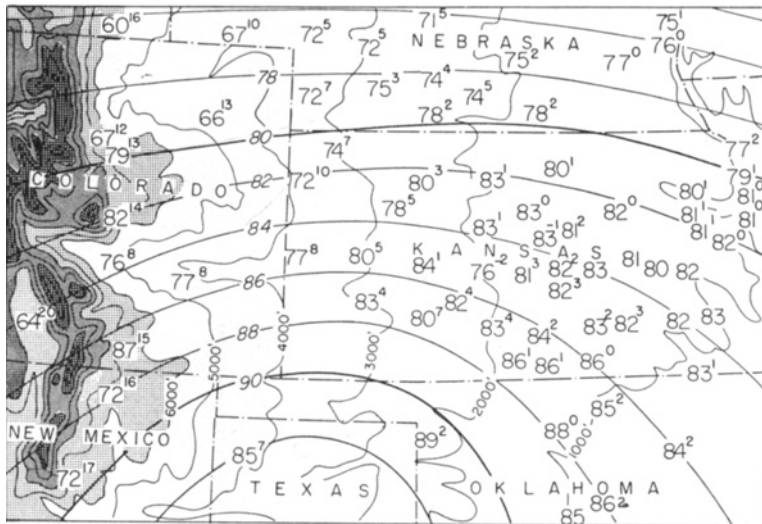


Fig. 12. Distribution of mean station temperature and the smoothed isotherms of sea-level temperature.

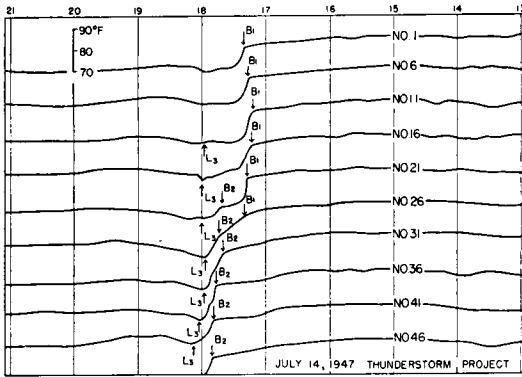


Fig. 13. Propagation of the temperature breaks over the Thunderstorm Project stations.

10° F. When we plot the temperature values on the hourly meso-scale chart, for instance, the amount of correction mentioned above must be added to the temperatures on the trace.

The second approximation is the correction of the value of T_1 , the diurnal variation. This is based on the fact that the variation is very large on the bare ground and small on the water. These local effects must be eliminated if possible. To make the correction easier, the smoothed isotherms may be drawn for the maximum and minimum temperatures, and they are corrected.

Experience shows that the mean value

correction is enough for the meso-analysis, and the correction to the diurnal variation is not always necessary.

In the meso-analysis of temperature, the thermograph traces must be used together with the corrected temperature values. Looking at the traces from each station, the points of break, maximum and minimum are checked first. The significant points are then termed as $B_1, B_2, \dots, L_1, L_2, \dots, H_1, H_2, \dots$, in which the numbers 1, 2, ... indicate the numbering of the disturbances by which the significant points are produced.

In Fig. 13, the breaks and the minimum temperatures are indicated on the traces from the Thunderstorm Project stations. The distance from stations No. 1 to No. 46 is 18 miles. When the temperature break travelled in this short distance, B_1 dissipated and B_2 appeared. It happens sometimes, when the distance between stations is large, that the significant points are very difficult to follow from station to station. In the micro-analysis, such breaks will appear to be double or triple lines, but in the meso-analysis no such fine structure can be shown.

For each significant point on the time-section isochrone charts are made. Then, the time-section can be converted into the space-section running through each station. An example is shown in Fig. 14, in which the traces are so oriented that time increases toward the per-

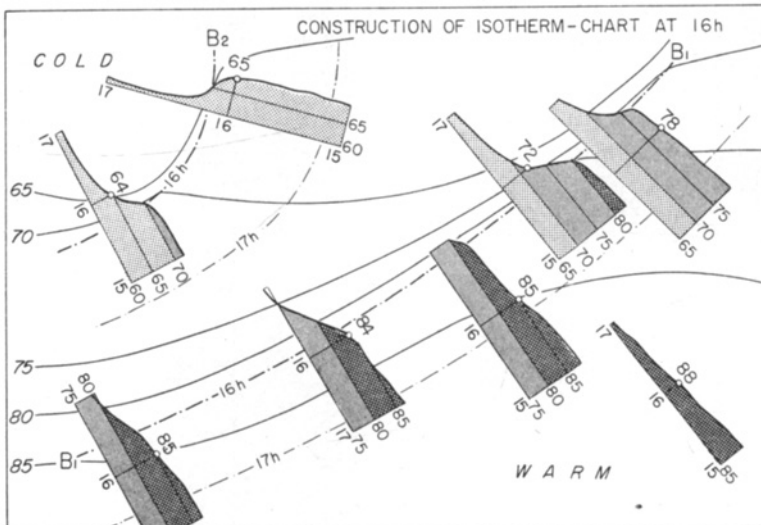


Fig. 14. Arrangement of the thermograph traces for the construction of an isotherm chart.

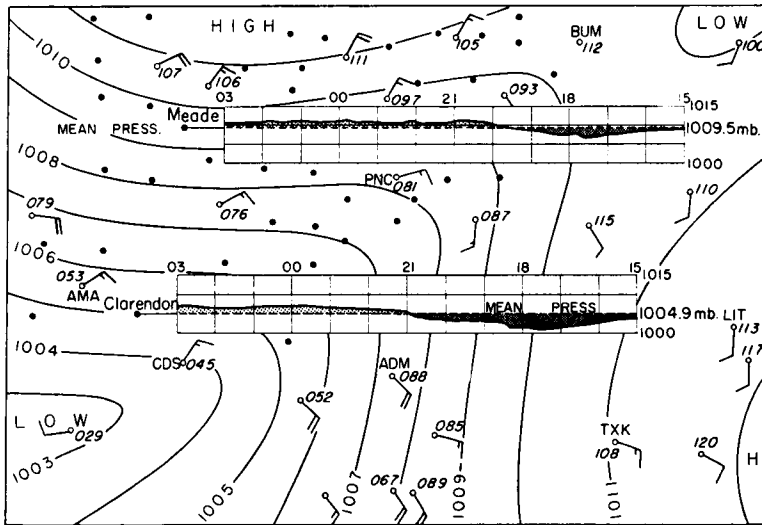


Fig. 15. Chart used in the reduction of the barograph traces to sea-level.

pendicular to the isochrone for the map time. The length of the trace corresponding to one hour is equal to the displacement of the isochrone in one hour. The traces are very helpful in determining the interval of the isotherms on the chart. The area under the trace is stippled by the different tones. They will help the drawing of the isotherms and their spacing. In the actual analysis, several different colors can be used, which show the temperatures 50—55, 55—60, 60—65, 65—70, 70—75, 75—80, . . .

Examples of the temperature analyses will be seen in sections 7 and 8.

6. Analysis of pressure

The barograph traces from the stations in the area of meso-analysis are the most important material we should have. As has been mentioned in the chapter section 2 of the time and the space section, the barograph traces from the Severe Storm Research Unit, U.S. Weather Bureau are used.

By using these traces, the writer tried to make sea-level charts. Unfortunately, most of the barograph stations have neither thermographs nor mercury barometers by which the station pressure could be obtained. Moreover, the elevation of the barograph stations is not accurately determined. Therefore, the formula of sea-level reduction is not available. Even if

we could have enough information for the sea-level reduction, we could not use the method of ordinary reduction; because a rise of the sea-level pressure occurs due to the drop in the station temperature, even if the station pressure remains unchanged. We are interested in the pressure pattern satisfying the original trace. This means that the traces must be reduced to sea-level without changing their shapes.

The reduction of the barograph traces from the Severe Storm Unit is done by drawing the isobars of the mean pressures from the teletype stations. As shown in Fig. 15, mean wind and mean pressure are mapped together. The isobars for the mean pressure show the mean sea-level pressure of each barograph station indicated by the dots. Barographs from Meade and Clarendon, for instance, are shown in the map, which are reduced to sea-level by shifting them upward or downward until the mean sea-level pressure, 1009.5 and 1004.9 mb, respectively, coincides with the mean pressure of the barograph traces. With the trace thus shifted, the sea-level pressures can be read directly on the pressure scale.

With a similar technique, shown in Fig. 14, the pressure values and the traces are used for the construction of the isobar chart. Another technique of changing the time section into the space section is provided. As will be seen in

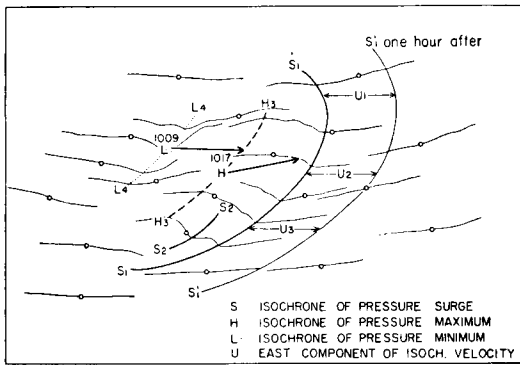


Fig. 16. Arrangement of the barograph traces for analysis of the pressure field.

Fig. 16, the isochrones for the time of the analysis are drawn first, which are Surge 1, Surge 2, High 3, Low 4. Making use of the characteristic that the eastward component of the displacement U_1 , U_2 , U_3 of the isochrone of the surge are similar, we enter the barograms on the chart keeping the barograph horizontal but with time increasing to the left. The length of the barograms in one hour is equal to the length of U . In the area where the pressure falls, the traces on the chart will increase eastward, so that the tendencies can be known immediately. When we enter the traces on the chart, some adjustments must be done so that the significant points come on the isochrones. Most of the recent analyses by the writer were done by using this technique.

When we examine the significant points on the original traces for squall-line systems, certain characteristics are apparent in many of them. Five different stages of the pressure profile of a rapidly moving squall-line thunderstorm high are shown in Fig. 17. The traces are characterized by the "pressure surge", "thunderstorm high", "pressure drop" and "wake depression". These disturbances are superimposed upon the undisturbed field. The deviation from the undisturbed pressure field is termed "the pressure excess," which may have either a positive or a negative sign.

Figure 18 shows how these characteristics are related to the horizontal and the vertical structure of the squall-line thunderstorm. The high-momentum air aloft is cooled and brought down by the downdraft, and spreads over the ground forming a large thunderstorm high. The descending speed of the downdraft will

contribute to the increment of the horizontal momentum. Meanwhile, the pressure gradient produced by the downdraft itself will accelerate the descending air before it reaches the ground. Even if the wind aloft is very light, it will be understood that the downdraft gust has a large speed at which it spreads out.

A mass of high-speed air following the pressure surge line will act much as if it were a solid body moving in a fluid. The wake flow is induced in the rear of the thunderstorm high if that happens to be the prevailing downwind side for low-level winds. The low pressure area thus produced is termed "the wake depression". Usually, the depression appears in the mature stage of a squall-line, forming, with the thunderstorm high, a positive and negative pressure dipole. If the winds in the low levels around the thunderstorm are moving in the same direction but faster than the pressure surge line, the wake depression will be found ahead of the thunderstorm.

When the system is changing rapidly, the change in the system itself will contribute to the tendency. To analyze such a case, the isobar charts for both undisturbed pressure and the excess pressure are made independently and they are superimposed. Fig. 19 was made in such process. The dashed isobars passing through the disturbed area show the undisturbed isobars of 1010 and 1008 mb.

The separation of the pressure excess from the original traces must be done very carefully. After the separation, the amount of the pressure excess for each barograph station is plotted on the chart. In Fig. 20, the heavy isobars are envelopes of the maximum amount of the

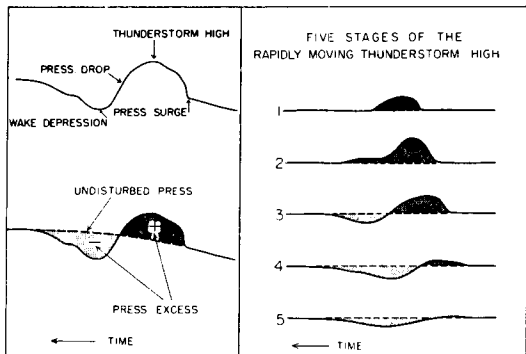


Fig. 17. Schematic diagram of the barograph trace for a squall-line thunderstorm. Time runs from right to left.

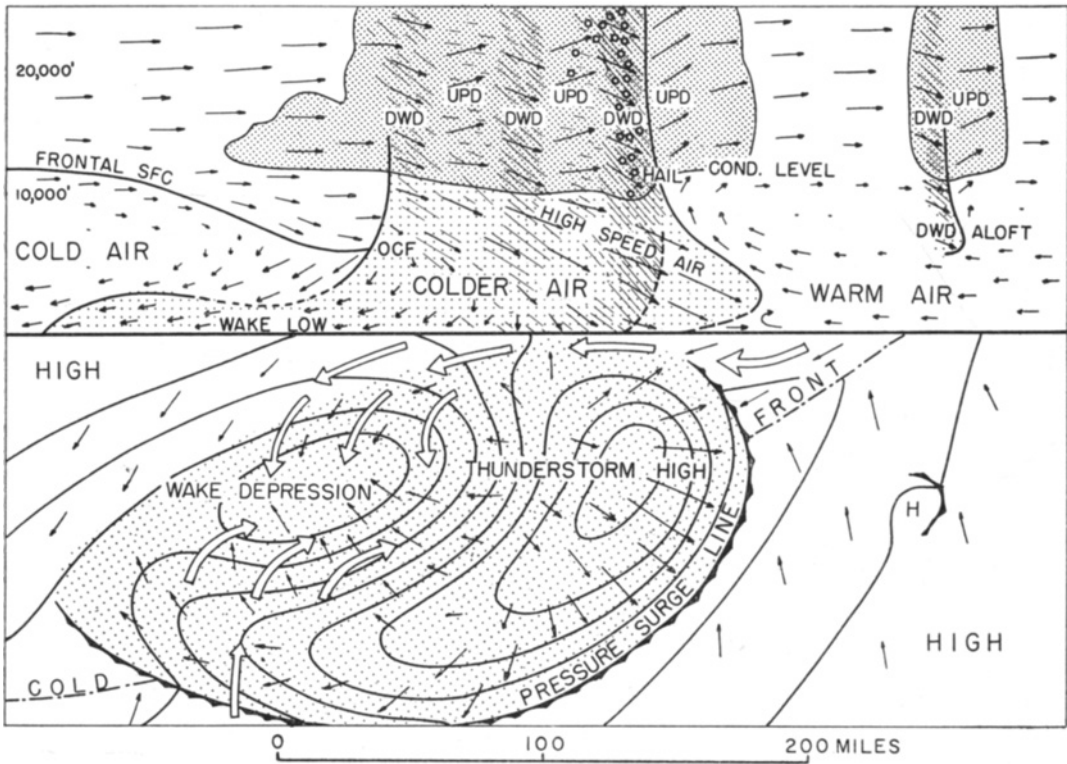


Fig. 18. Schematic section through a squall-line thunderstorm, and illustration of the wake depression.

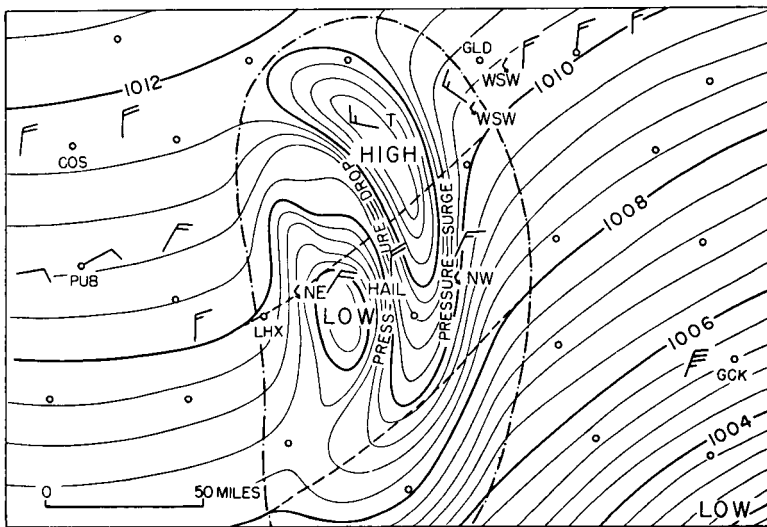


Fig. 19. Details of a meso-analysis of a rapidly moving thunderstorm high.

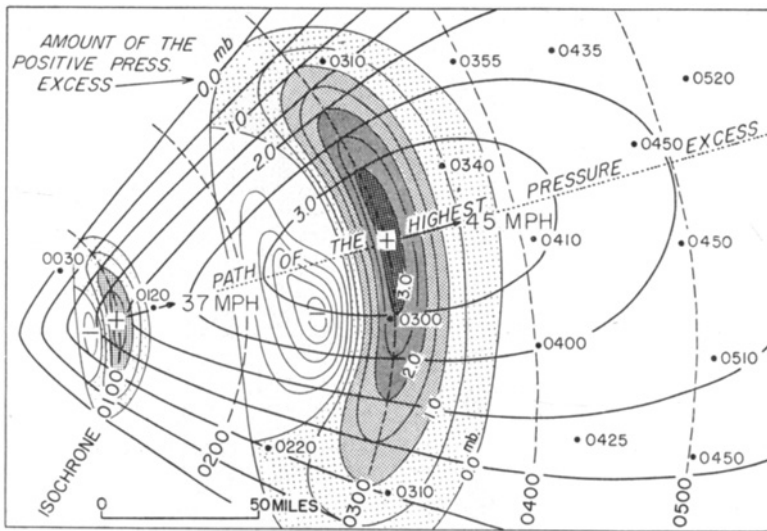


Fig. 20. Isobars of pressure excess.

pressure excess as it swept over the map. The analyses show that the system started to develop between 0000 and 0100 CST. Within three hours, the maximum pressure excess reached more than 3 mb. From these isochrones and the isobars for the excess pressure, the amount and the location of the highest point of the excess pressure are known for any hour. The isobars of the excess pressure for 0300 and 0100 CST are contoured on the chart. The 0300 isobars of pressure excess superimposed upon the undisturbed pressure chart produce the actual sea-level isobars in Fig. 19. Using a similar method, the negative disturbances are analyzed.

7. Analysis of squall line of June 5—6, 1953

In the afternoon and evening of June 5, a very strong squall line accompanied by heavy rains, hail and tornadoes swept over the entire state of Oklahoma and the southern portion of Kansas. Eleven tornadoes were reported. Hailstones of the size of golf balls piled up to a depth of seven inches on the highway north of Ardmore, Oklahoma (see index map, Fig. 21).

The tornadoes reported in the National Summary of the Climatological Data are shown in Fig. 22. The locations and times of the tornadoes indicate the existence of five tornado sequences. They are ABDC, EFG, HI, J, and KL. The events suggest the displacement

of a "tornado cyclone." BROOKS (1949, 1954) called the micro-low, intermediate in size between the regular cyclone and the tornado funnel within it, "the tornado cyclone". FULKS (unpublished) emphasized the initiation of the upper vortex in his model of tornado initiation.

The writer considered from the distribution of the tornadoes shown in Fig. 22, that there exists a tornado cyclone inside of which tornadoes develop periodically. The paths of the five tornado cyclones related to the five tornado sequences of June 5 are shown in Fig. 23. These tornado cyclones are fixed also by the traces from the barograph stations available. To know the relation between the tornadoes and the pressure surge, the isochrones of the surge are shown on the same chart. It will be seen that the tornado cyclones No. 1 and No. 2 were initiated before the pressure-surge line was organized.

Hourly Meso-synoptic Chart. Hourly meso-synoptic charts are made from 14 h to 24 h of June 5, and they are shown in Figs 24—34. At 1400, tornado cyclone No. 1 is already seen near the western border of Oklahoma and Texas. About 30 minutes prior to the map time, tornado clouds were observed, with one touching the ground. On the chart, the isobars are drawn for every one mb, and the isotherms for every 2° F. The meteorological conditions

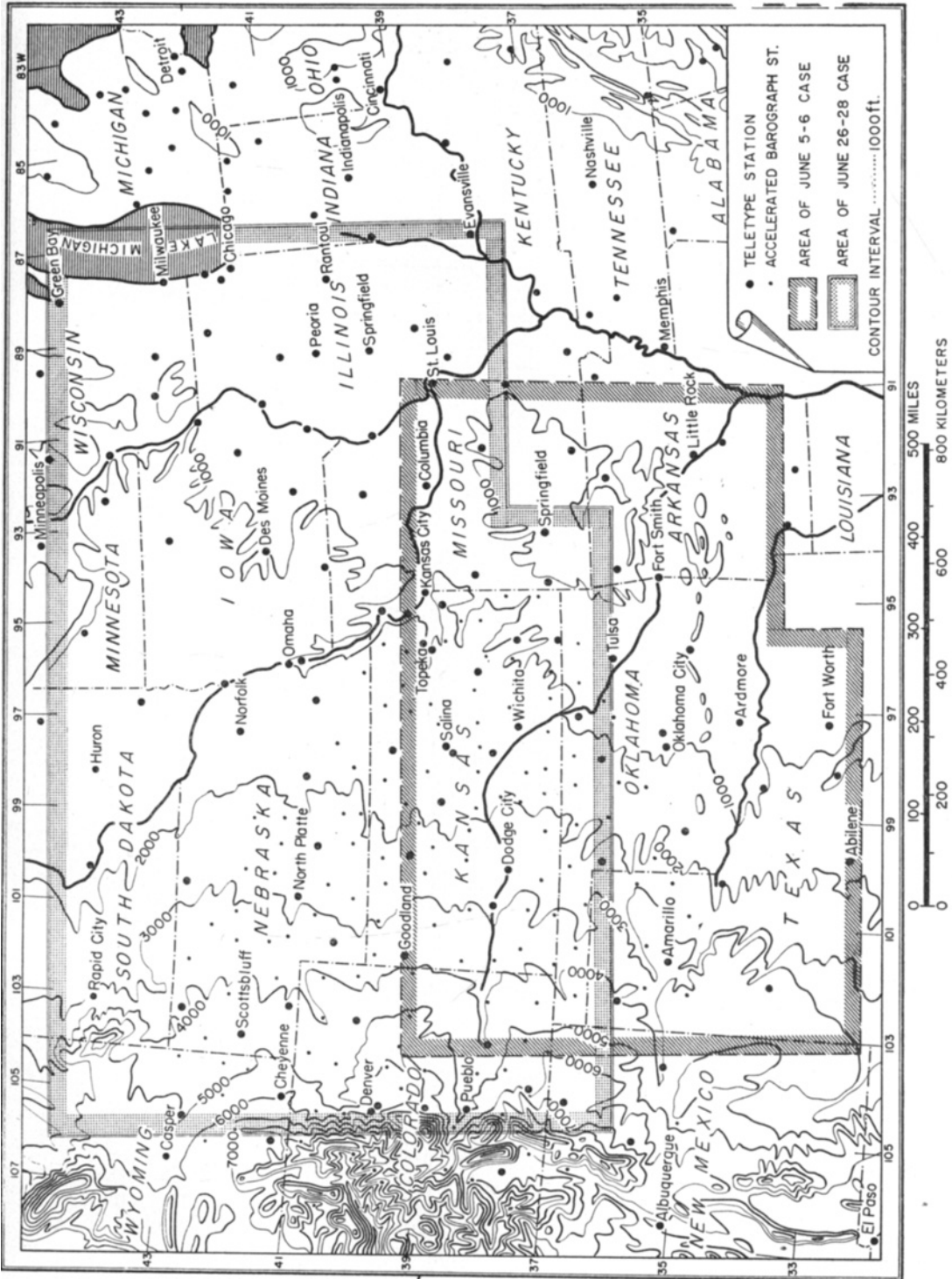
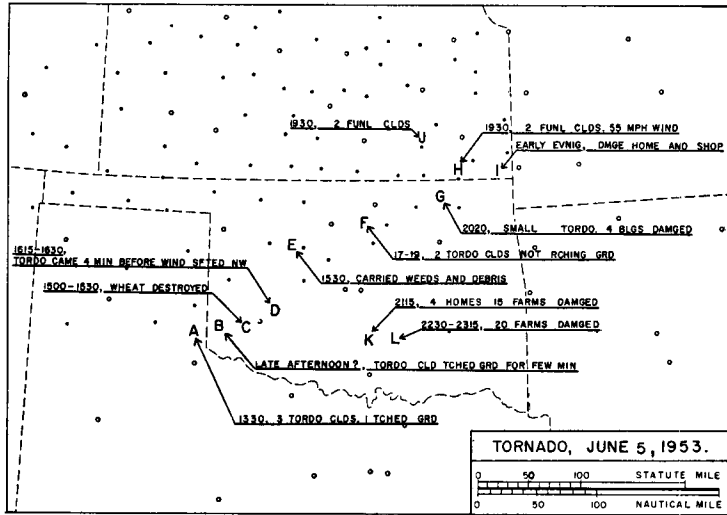


Fig. 21. Map of areas used in analysis of the two cases.



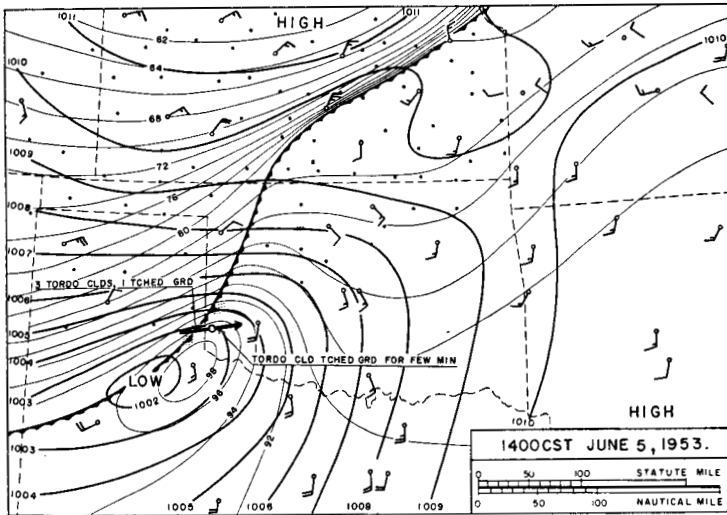


Fig. 24.

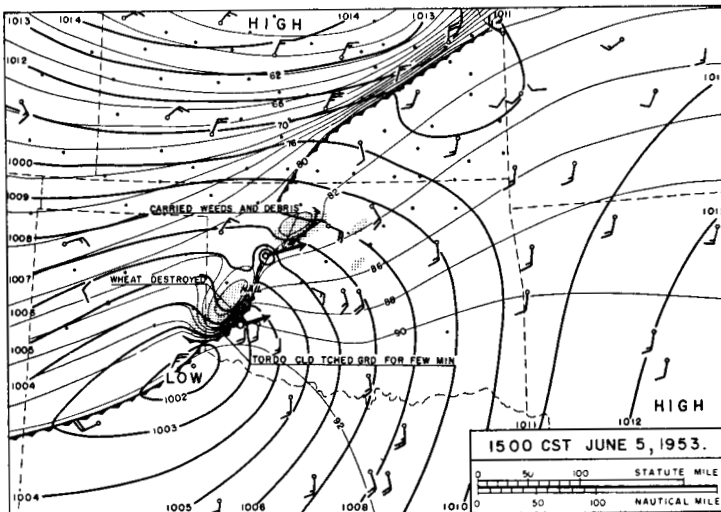


Fig. 25.

tornado in the north was engulfed in the cold air. Between 1615 and 1630, the tornado in the south came 4 minutes before the wind shifted to northwest. This means that the southern tornado moved slightly earlier than the surge line.

By 17 h, tornado No. 2 travelled east-north-eastward above the cold dome. A tornado

Tellus VII (1955), 4

2-508897

cloud not reaching the ground was reported. Probably, the underlying cold air prevented the dipping of the funnel cloud down to the ground. Usually, a horizontal vortex inside the upper layer of a twofluid system sucks up the lower fluid, in a similar manner to that we see on the sea surface in a hurricane center. This situation continued till 18 h.

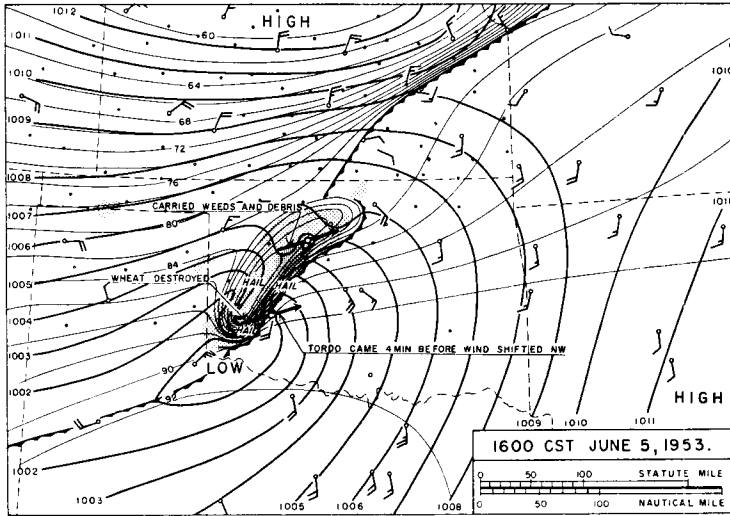


Fig. 26.

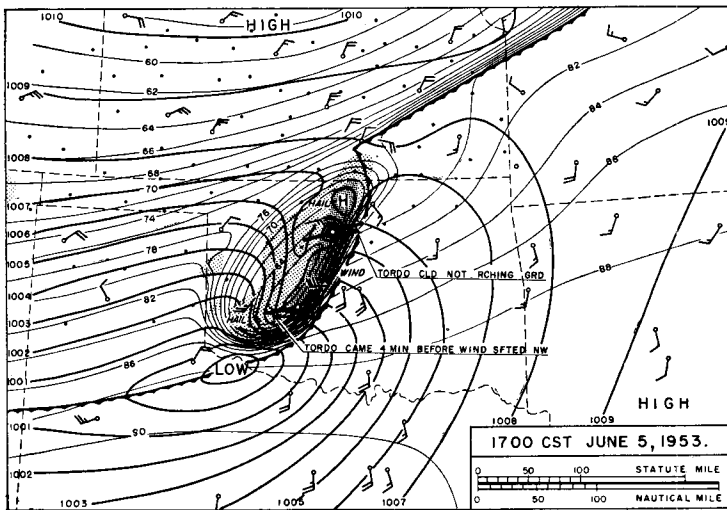


Fig. 27.

At 19 h, another small system entered into the map area from the west. Two new tornadoes (Nos 3 and 4) appeared in the northern part of the big thunderstorm high. While the tornado cyclone No. 2 is travelling over the cold dome during this hour the tornado funnel apparently managed to reach the ground. In the Climatological Data (1953), it is reported

that four buildings were damaged or destroyed. The funnel observed appeared to be smaller than most tornadoes. This tornado would have spent much energy to make a vortex in the cold air.

A wake trough had developed by 2100, and tornado cyclone No. 5 appeared inside the cold air to the south. Prior to the appearance

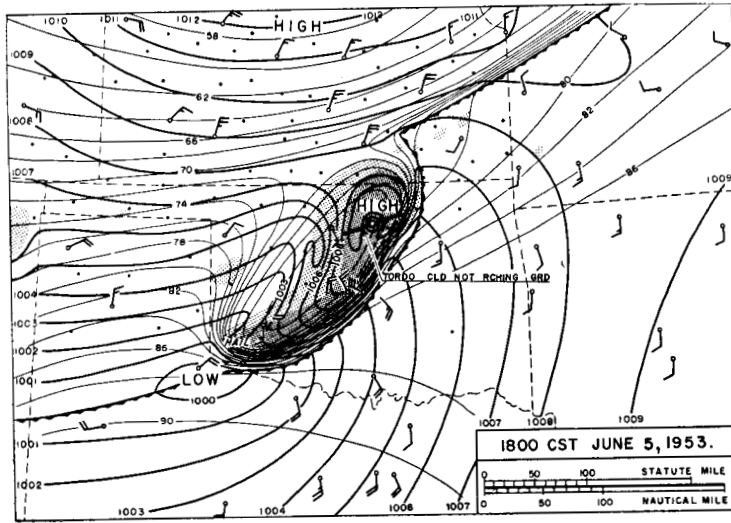


Fig. 28.

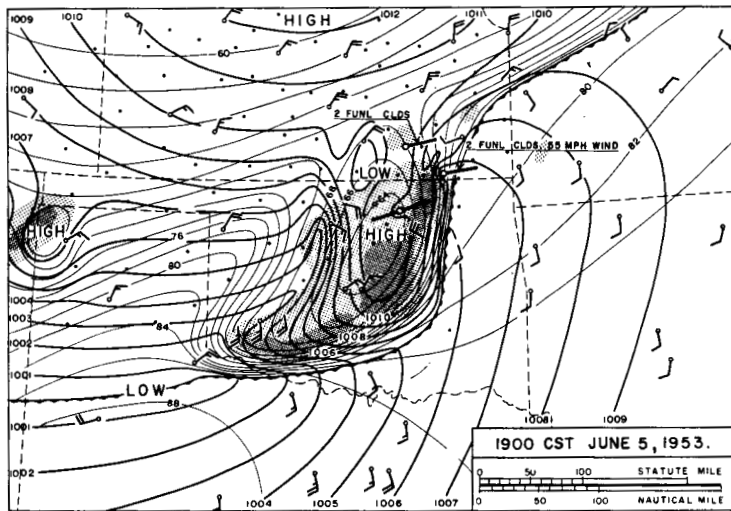


Fig. 29.

of the tornado cyclone, hail was reported in the area where the initiation of the cyclone probably occurred. Strong hail moved eastward with the tornado cyclone. Hailstones of 1/2 to 1 inch in diameter piled up seven inches deep on the highway. A wake depression center, having a higher temperature inside, appeared at 22 h. By this time, the

Tellus VII (1955), 4

squall-line activity became weaker; meanwhile, the surge line moved far eastward from the rain areas.

At 2300 and 0000 next day, the thunderstorm high associated with the main storm became weaker. The thunderstorm high in the north was intensified by the heavy rain in that area. A well developed wake depression is seen in

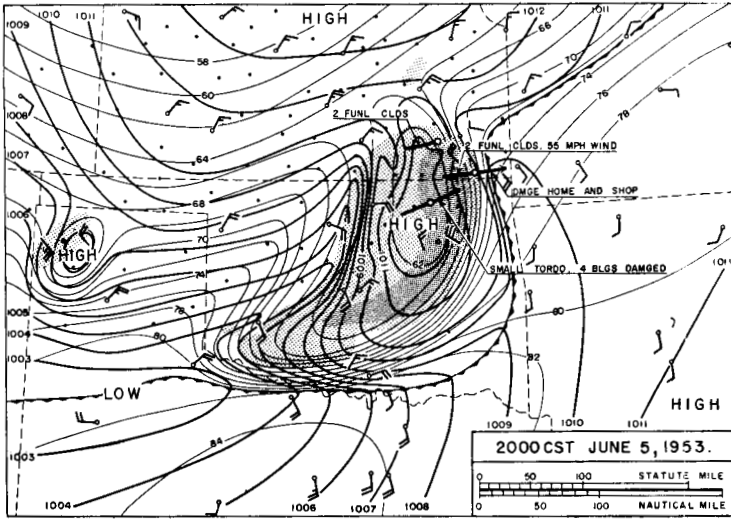


Fig. 30.

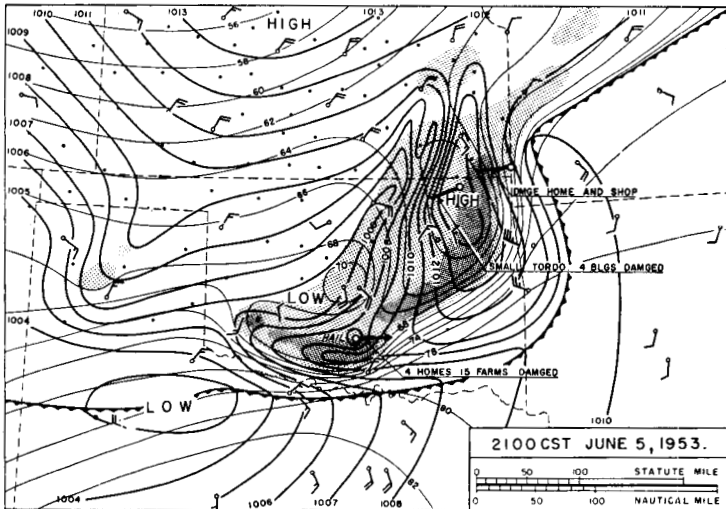


Fig. 31.

the rear. Hail is continuing in southern Oklahoma, but no tornadoes are reported in the storm areas.

Condition of the Tornado Initiation. — Meteorological conditions which gave rise to the development of the tornado sequence No. 1 are shown in Fig. 35. The tornado was reported at 1300 in the Texas Panhandle near the Okla-

homa border. Amarillo radar reported "PPI NO ECHO" at 1305, then at 1335, "scattered circular echo 8 miles diameter" is reported to the south of the tornado, which had been observed as a tornado by that time. The echo moved north-eastward developing into an elliptical, scattered, 20 by 8 mile echo. At Childress, thundering cumuli were observed

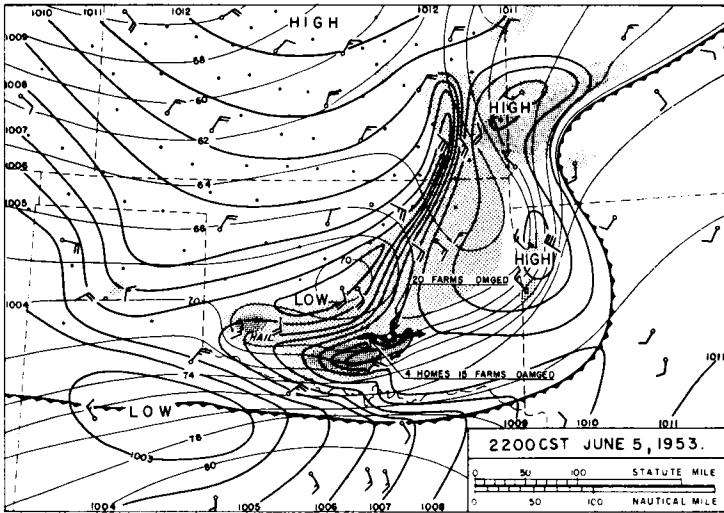


Fig. 32.

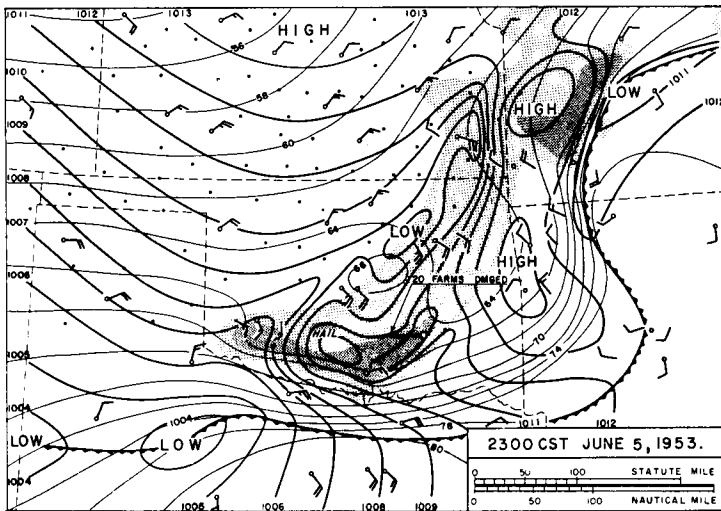


Fig. 33.

at 1230, then at 1330, when the tornado was reported, a rain shower was visible to the north. A pilot reported, at 1219, that he met light turbulence in the line of cumulus oriented SW—NE on the Oklahoma and Texas border.

From the traces of the three barograph stations in the area, no indication of pressure surge was seen, which might have moved into

Tellus VII (1955), 4

the tornado area from the west. From these facts the space section of the clouds and of the pressure from CDS to TUL in Fig. 36 are constructed. The tornado cyclone is believed to have been initiated at 1330 in the area where an isolated shower of 8 miles in diameter existed. No appreciable pressure-surge lines are recognized in that area. One or two hours

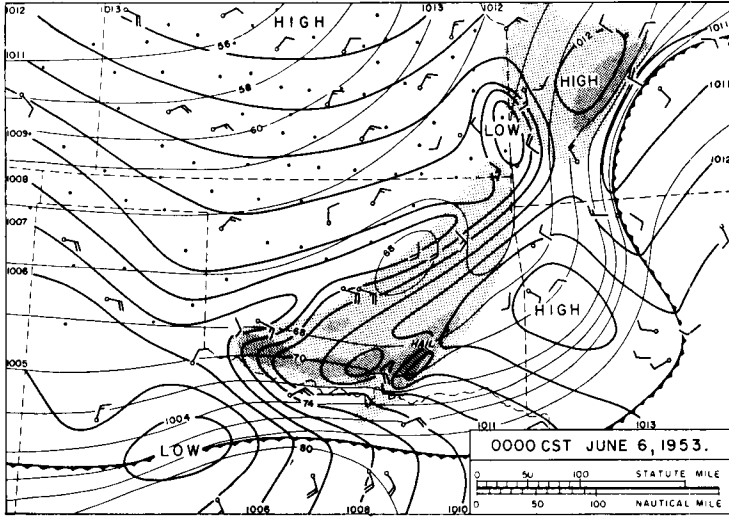


Fig. 34.

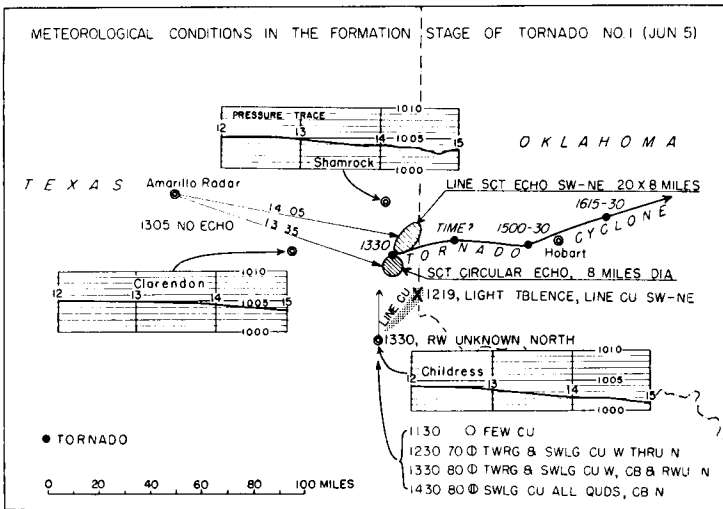


Fig. 35. Meteorological conditions in the formation stage of tornado No. 1.

after the development of the tornado, a surge line became intense.

The conditions of the initiation of the tornado cyclone No. 2 are shown in the chart to the right in Fig. 36. In this case, however, the surge line moved faster than the tornado. Such a case is unfavourable for the extension of the funnel cloud down to the ground. Therefore, the tornadoes of this sequence

either were very small or did not reach the ground.

8. Analysis of squall line of June 27, 1953

In this study, the meso-analyses were carried out in a large area of 600 by 1000 miles. Hourly charts were made for a 36-hour period, seven of which are presented.

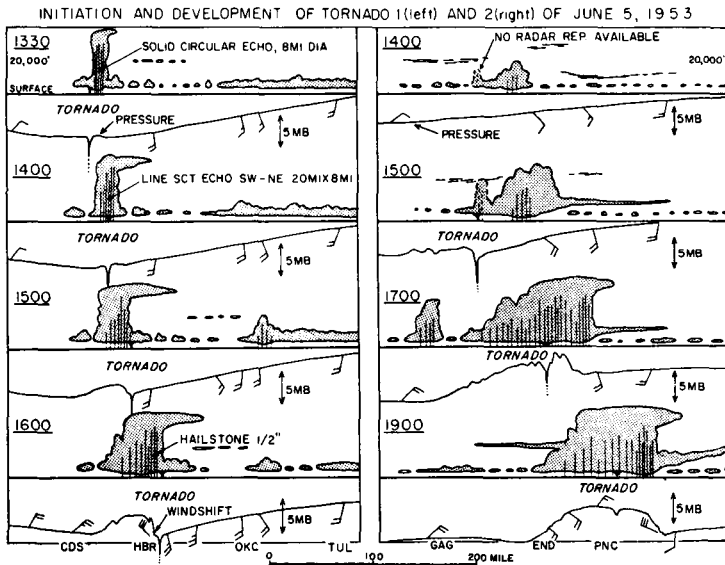


Fig. 36. Schematic section of cloud and pressure related to the tornado initiation.

At 15 h on the 27th (Fig. 37), a post-mature thunderstorm high was travelling over the Chicago area. It was followed by a very deep wake depression, having a pressure drop of about 8 mb. Along the cold front passing across the middle portion of Kansas, several rain showers and thunderstorm highs were being formed. The isotherms for every 2° F show no discontinuity at the front of the cold air. One hour later, at 16 h (Fig. 38), a strong shower accompanied by a tornado developed in southwestern Iowa. In the chart, the barograph traces are entered in a manner similar to that of Fig. 16. These traces show the gradual drop in pressure east of the front.

The thunderstorm high over the Chicago area became weak, reaching the "Stage 4" of Fig. 17. The barograph traces showed an appreciable pressure surge. Three thunderstorm highs located along the cold front have not yet developed a wake depression. They are now in "Stage 1." The tornado in Iowa is moving almost at the same speed as the pressure surge. By 17 h the trough associated with the front has deepened in some places in the expected positions of wake depressions.

By 18 h pressure-surge lines of the three thunderstorm highs were combined into a lone one. Heavy thunderstorm rains are moving behind the surge. On the other hand, the

thunderstorm high near Chicago has reached the "Stage 5", in which the pressure surge dissipates and the wake depression remains. Tornadoes are still active in Iowa.

The pressure-surge lines moved far to the east from the cold front. According to the diurnal variation of the pressure, which is positive at 19 h, a gradual rise in pressure is seen to the east of the surge line.

A wake depression in Iowa became pronounced at 20 h. The rapid movement of the surge line left the rain areas far to the west.

The large thunderstorm highs reached the post-mature stage by 21 h. The characteristics of this stage are the separation of the lines of pressure surge, temperature break, and the beginning of rains. In case of a strong daytime squall line, these three lines occur almost at the same time. In the night-time squall lines, however, the surface inversion prevents the sinking of the cold-dome air down to the ground. Especially in the post-mature stage, the absence of rain immediately behind the surge line means an absence of precipitation cooling following the pressure surge. It is usual in this stage that the temperature breaks one half to one hour after the pressure has surged. It will be seen in the chart at 21 h, that the surge line is about 30 to 40 miles ahead of the line of the temperature break.

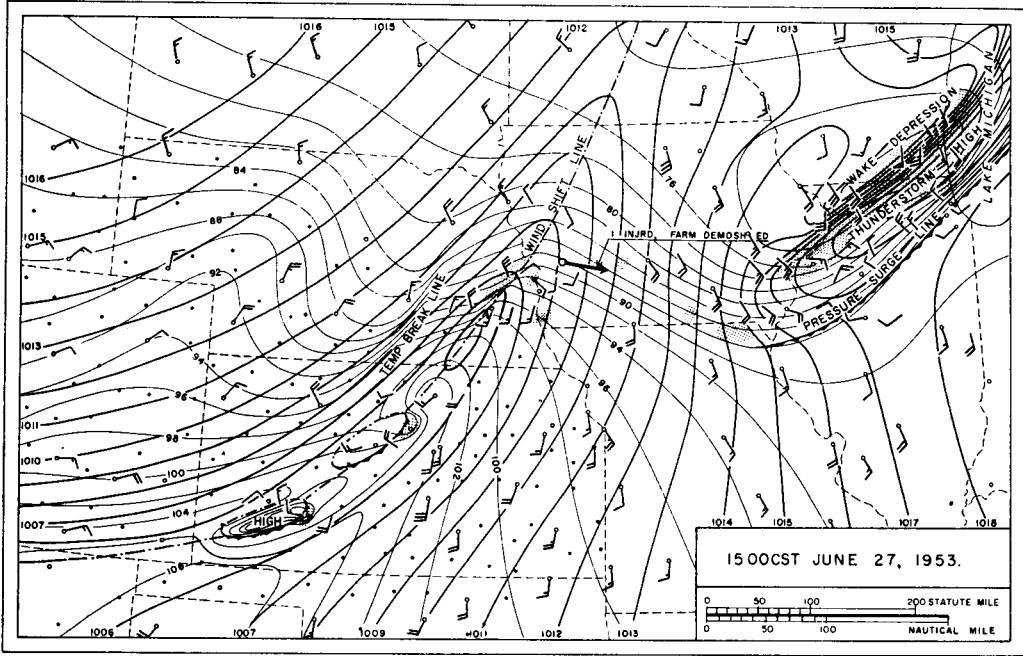


Fig. 37.

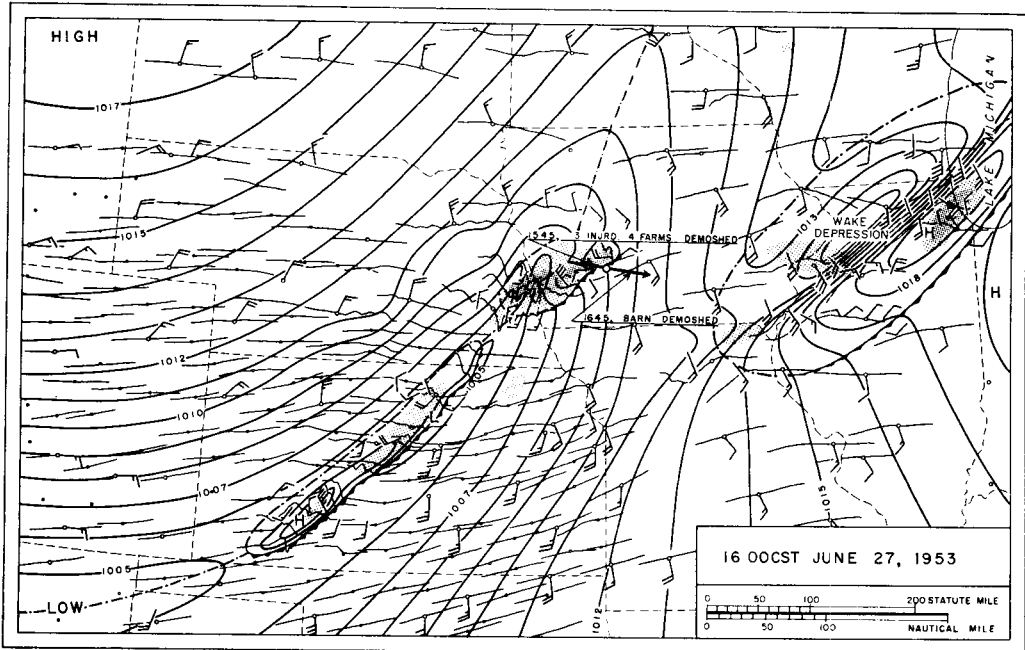


Fig. 38.

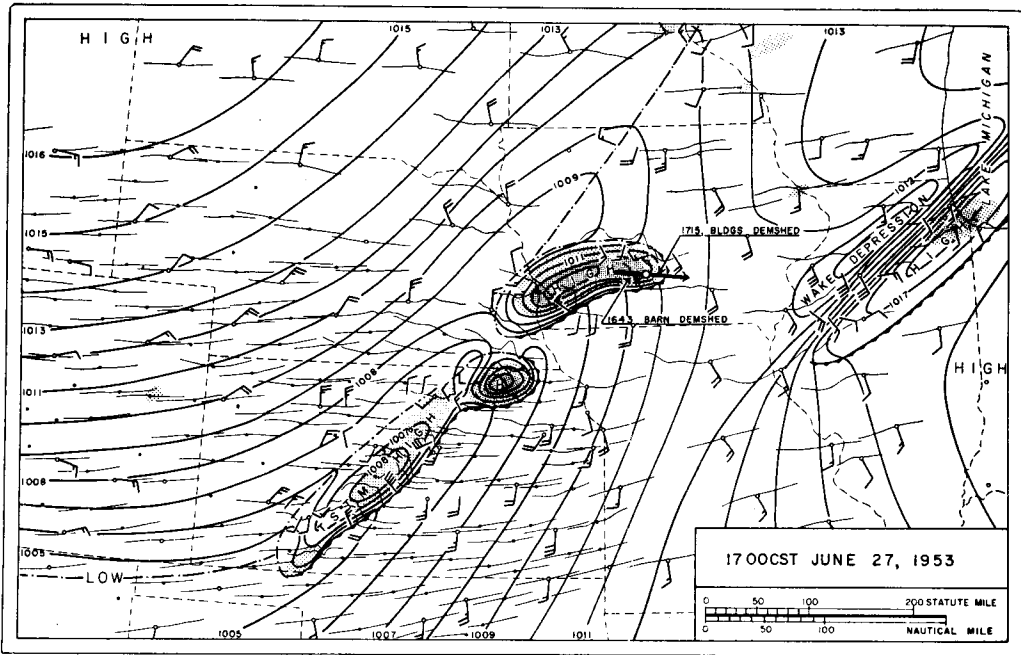


Fig. 39.

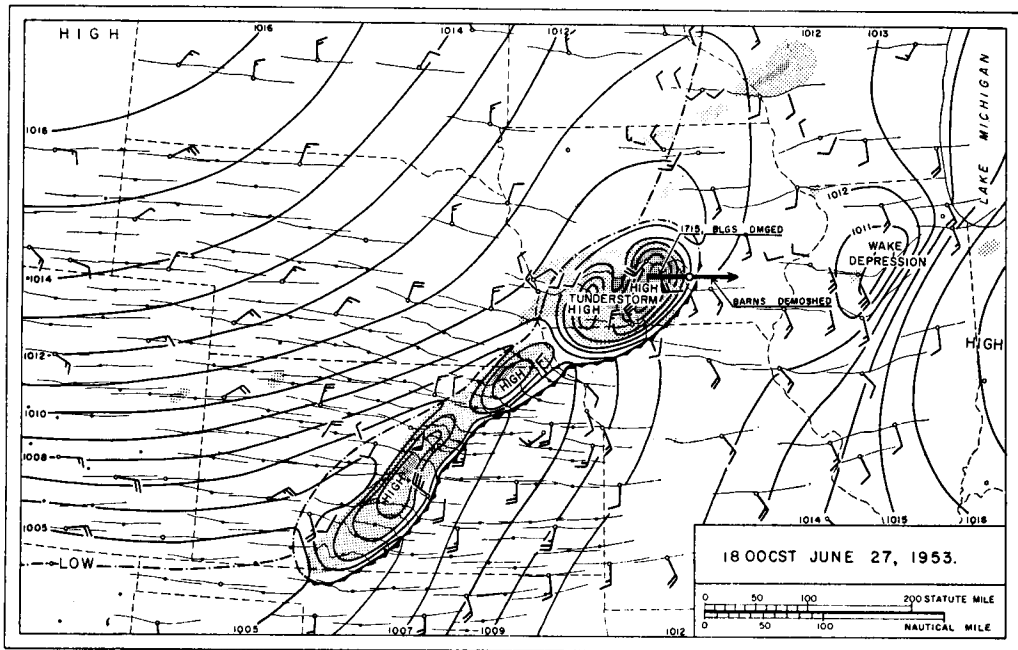


Fig. 40.

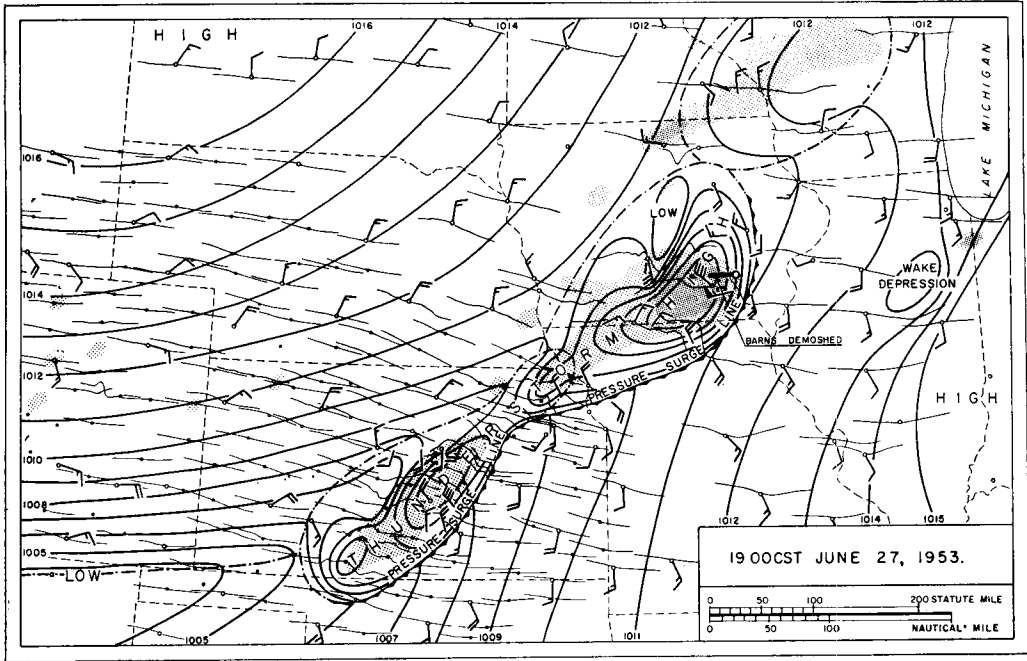


Fig. 41.

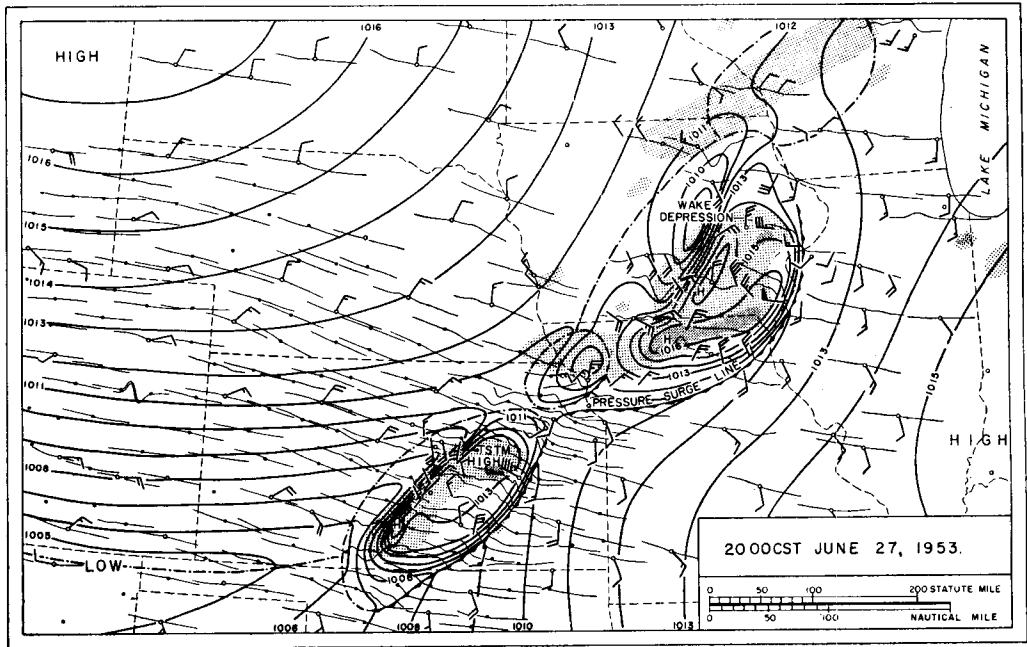


Fig. 42.

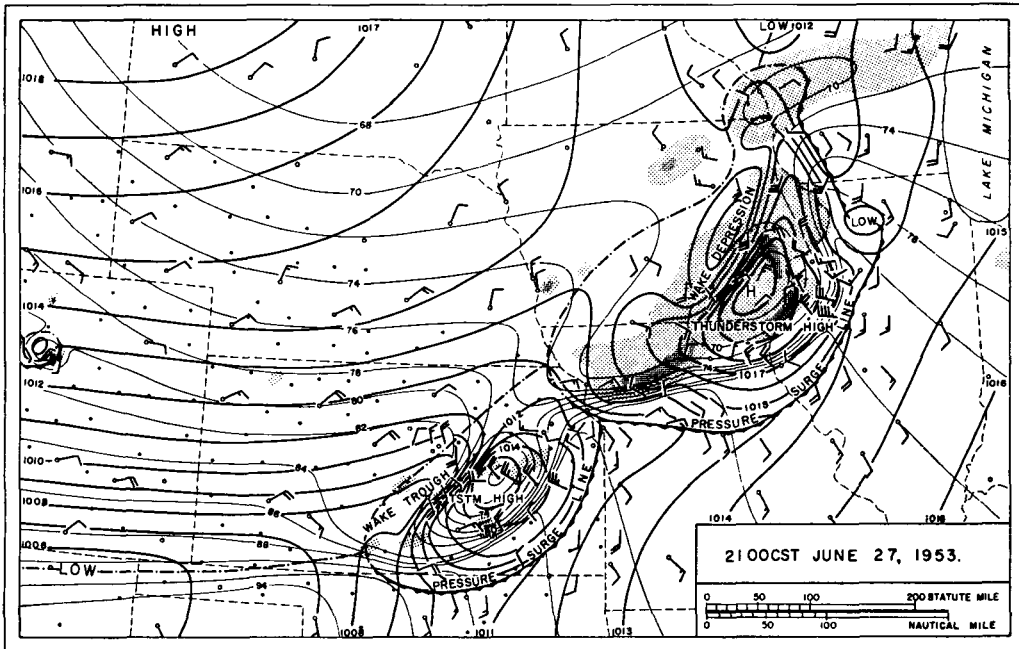


Fig. 43.

Meteorological conditions of the early stage of the tornado occurrence in Iowa are shown in Fig. 44. Norfolk, Nebraska, radar reported a line echo at 1440. Within one hour it developed into a large echo, bringing in a heavy rain represented by the isohyets for 1500—1600. The tornado was reported at 1545 at the position shown on the chart. It can be considered that the tornado cyclone associated with the tornado would have been formed at 1500 or 1530. The initiation of the tornado cyclone would be related to the heavy rain of 0.86° seen in the figure north of the cyclone path. Pierce (13) has pointed out that tornadoes tend to form at the southwestern part of a large thunderstorm, as suggested also by this case. From the fact that we had no rain before 15 h, except 0.02° at Omaha, it is concluded that this tornado cyclone must be related to a very early stage of the squall-line development.

The time section for Omaha shows the pressure surge at 1530 and the temperature break at 1450. The station is so far from the tornado area that we cannot expect to find any further information about the tornado.

Tellus VII (1955), 4

9. Some representations in color

The cloud chart at 21 h, June 27, 1953 is shown in Plate 1. The blue bands indicate vertical cross-sections up to 30,000 ft. which pass through the teletype stations. The shapes of the clouds were estimated by changing the time section, such as in Fig. 1, for example, into a space section. To make the relative positions of the clouds with the surface systems clear, the surface winds and isobars are shown in the areas outside of the blue bands. It will be seen that the developed squall line thunderclouds are moving over the thunderstorm highs shown in pink. Surface rains of the past hour are shown by the blue areas. The lightning, schematically represented by red arrows, and the rain inside the clouds (blue vertical lines) is also entered. This chart was made for demonstration purposes; however, the antecedent charts now to be examined show the developments leading up to this peak of squall-line activity.

With the technique introduced in the section on wind analysis, divergence and convergence were computed for the hours 15 and 20, June

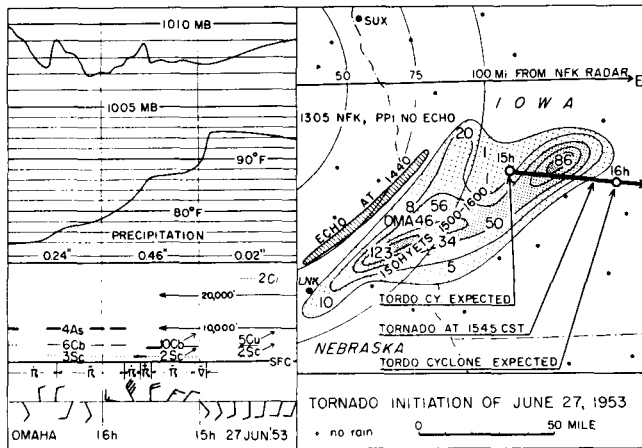


Fig. 44. Meteorological conditions of the tornado initiation in Iowa.

27, 1953. In Plates 2 and 3, divergence areas are represented by different intensities of red, while convergence is indicated in the blue areas. In the chart at 15 h (Plate 2), a convergence zone is seen along the cold front. Five hours later, at 20 h, four thunderstorm highs had developed. The most important feature of the divergence pattern in the chart is the very high values of the velocity divergence existing inside the meso-scale thunderstorm highs. It is known by the "Thunderstorm Project" that a very large divergence exists inside the micro-scale thunderstorm high. The meso-scale divergence of 10 to $60 \times 10^{-3}/\text{sec}$ is shown for the first time by this analysis. Actually, the thunderstorm highs are increasing despite the large value of divergence near the ground. This fact suggests the existence of a very strong converging flow aloft, which must overcompensate the surface divergence as shown also to be the case in individual cells examined by Byers and Hull (7). It will be natural to consider that the inversion layers which might have existed originally should be destroyed by the vertical motion.

A schematical section of the squall line at 21 h is shown in Plate 4. In the upper chart representing the soundings, the area between the temperature (T) and dew point (T_d) curves is colored in pink. The pressure-surge line to the right is moving eastward at the rate of 55 knots. The cold front surface fixed by the ascent reached the 10,000 foot level. Location of the surface cold-front, which is not visible

in the surface chart, is determined by extrapolating the profiles of undisturbed pressure on both sides of the thunderstorm high into the thunderstorm area as indicated in the space section of pressure in the center chart. Winds in the lower chart are the ones *relative* to the system which is moving eastward at the rate of 30 knots, at which speed the thunderstorm high is moving. The front of the cold thunderstorm air, moving at 55 knots eastward, is faster by as much as 25 knots than the speed of the high. It will be seen that the upper winds obtain some additional momentum through their descending motion and the effect of the pressure gradient near the surface. Inside the wake depression, the air is accelerated eastward due to the wake friction of the thunderstorm high. The main low-level flow relative to the thunderstorm high is in the sense that the wake is to the west of the thunderstorm mass.

10. Conclusions

The detailed analysis methods developed by the author in Japan, extended and refined in their application to the Central United States, give as true a picture of meso-scale phenomena as can possibly be obtained from the data and records. The scheme of analysis described enables one to make inferences concerning the magnitudes and times of weather changes or events not specifically given in the data as, for example, in the crude reporting of climatological co-operative stations. Meso-scale pat-

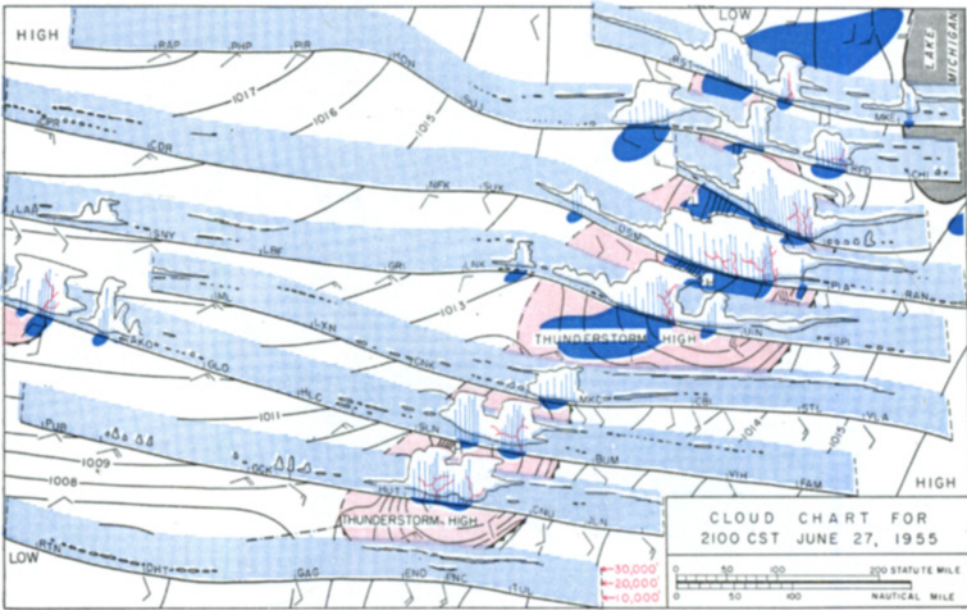
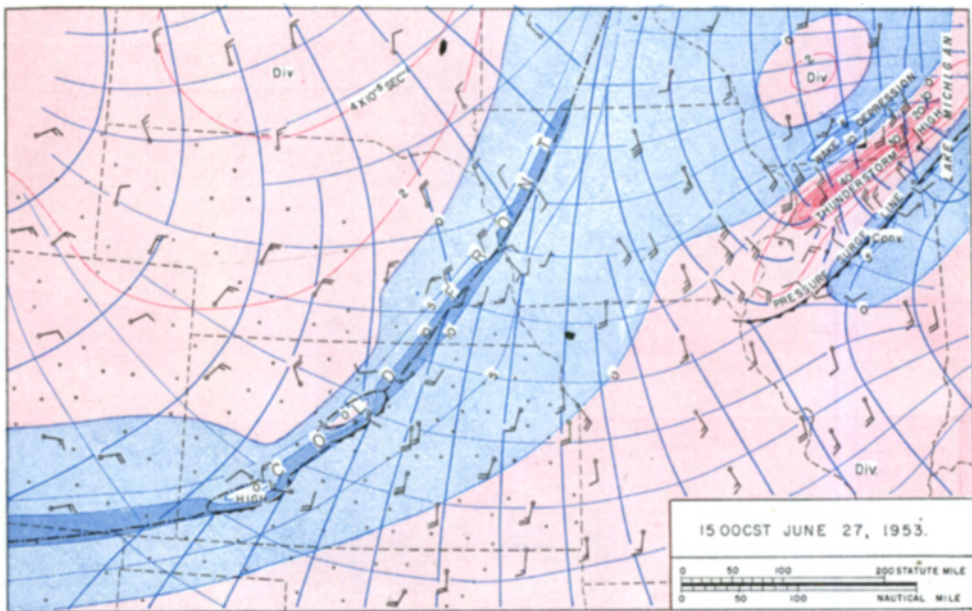


Plate I. Squall-line clouds and weather at 2100, June 27, 1953.



DIV IN 10^{-3} PER SEC

Plate II. Divergence and convergence pattern for 1500, June 27, 1953.

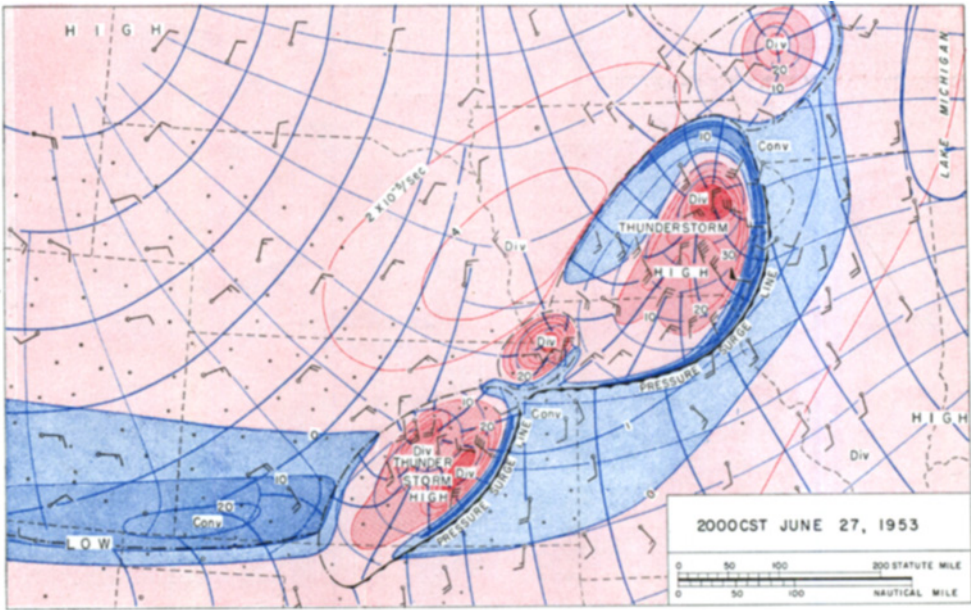


Plate III. Divergence and convergence pattern for 2000, June 27, 1953.

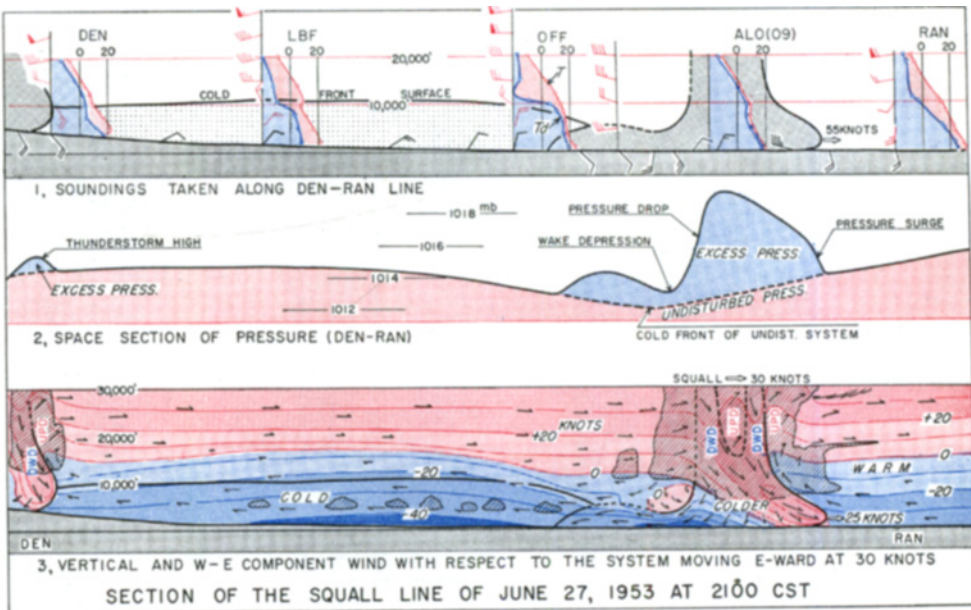


Plate IV. East-west cross section of the squall-line of June 27, 1953 at 2100 CST.

terms such as squall lines lead themselves admirably to this type of interpretation.

In the analysis of the squall line of June 5—6, 1953 five tornado sequences were noted, each associated with an intense tornado cyclone in which the tornado funnels intermittently appeared. This intense system of storms was initiated *before* a pressure-surge line was organized. This suggests the futility of seeking a "trigger" mechanism in the pressure field at the initial stage.

The analysis shows that tornado cyclones can move either faster or slower than the pressure-surge line. In the slower moving case, the tornado cyclone becomes surrounded in the low levels by cold air of the thunderstorm high and the penetration of tornado funnels down to the surface is inhibited.

A low pressure center or trough, much larger in dimensions than the tornado cyclone but much weaker, appears as the "wake depression". This depression was well marked in the second case analyzed, that of June 27, 1953. Another feature of this case was the lack of coincidence, during the night, of the lines of pressure surge, temperature break and beginning of rains. This appears to be characteristic of night thunderstorms and is explainable as an effect of the nocturnal inversion in preventing the downdraft and outflow from reaching the ground.

Colored charts and diagrams are an essential feature of the type of analysis treated here. In the interests of economy in printing, only a few maps are reproduced in color in this article. The charts in Plates 2 and 3 show the unusually high values of divergence (10 to $60 \cdot 10^{-5} \text{ sec}^{-1}$) obtained in this scale. The vertical analysis in Plate 4 demonstrates that the rapid displacements of the lines are in agreement with the winds above the frictional layer. This suggests that the speed does not

have to be explained by a mysterious upper impulse-type wave.

If the charts analyzed in this article were to be considered in the usual synoptic scale of 1:10,000,000 or less with stations 50 to 100 mi. (80 to 160 km) apart, a highly confusing picture would result. In drawing the isobars one could, of course, ignore the pressure report of a station that might happen to be in the thunderstorm high, the wake depression or, highly improbably, the tornado cyclone. But since the recognizable features of the true front are completely obliterated, its location on the map would be impossible to find.

In the short-period forecasting or extrapolation of the weather on the meso-synoptic scale, the complete data such as used in this paper are not available on a current basis, so it is necessary to rely on other tools. On this basis, the most helpful information is that to be obtained from a network of continually operating radar stations.

Acknowledgements

The study was carried out at the University of Chicago under the supervision of Dr Horace R. Byers, chairman of the Department of Meteorology. Sincere gratitude is expressed to Dr Byers for his kind guidance and comments in the development of the writer's mesoanalyses.

The writer wishes to express his thanks to Dr Morris Tepper, Severe Storm Research Unit, U.S. Weather Bureau, for making the traces from the Severe Storm Network available; to Mr Leslie Smith and Mr Lawrence M. Dye, National Weather Records Center for their kind help in the collection of the weather data; and to Dr George W. Platzman, University of Chicago, for his suggestions for the advancement of the studies. The writer is also very grateful to Mr Krishna Murti for his assistance in the analyses.

TABLE OF ABBREVIATIONS

(a) Station Names

ADM	Ardmore, Oklahoma	CHI	Chicago, Illinois	DBQ	Dubuque, Iowa
AKO	Akron, Colorado	*CLN	Clarendon, Texas	DDC	Dodge City, Kansas
ALO	Waterloo, Iowa	CNK	Concordia, Kansas	DEN	Denver, Colorado
BDF	Bradford, Illinois	CNU	Chanute, Kansas	DHT	Dalhart, Texas
BUM	Butler, Missouri	COS	Colorado Springs, Colorado	DSM	Des Moines, Iowa
CBI	Columbia, Missouri	CPR	Casper, Wyoming	END	Enid, Oklahoma
CDR	Chadron, Nebraska	DAL	Dallas, Texas	FAM	Farmington, Missouri
CDS	Childress, Texas			FLP	Flippin, Arkansas

FYV	Fayetteville, Arkansas	LXN	Lexington, Nebraska	RAP	Rapid City, South Dakota
GAG	Gage City, Oklahoma	*MKC	Kansas City, Missouri	RFD	Rockford, Illinois
GCK	Garden City, Kansas	MKE	Milwaukee, Wisconsin	RST	Rochester, Minnesota
GLD	Goodland, Kansas	MLC	McAlester, Oklahoma	RTN	Raton, New Mexico
GRB	Green Bay, Wisconsin	*MLI	Moline, Illinois	SBN	South Bend, Indiana
GRI	Grand Island, Nebraska	NFK	Norfolk, Nebraska	SGF	Springfield, Missouri
GSH	Goshen, Indiana	*NTA	Nowata, Oklahoma	*SHK	Shamrock, Texas
HBR	Hobart, Oklahoma	OFF	Offutt, Nebraska	*SLG	Seiling, Oklahoma
HLC	Hill City, Kansas	OKC	Oklahoma City, Oklahoma	SLN	Salina, Kansas
HON	Huron, South Dakota			SNY	Sidney, Nebraska
HUT	Hutchinson, Kansas	*OKN	Okeene, Oklahoma	SPI	Springfield, Illinois
IML	Imperial, Nebraska	OMA	Omaha, Nebraska	STL	St. Louis, Missouri
*IRK	Kirksville, Missouri	OTM	Ottumwa, Iowa	*STW	Stillwater, Oklahoma
JLN	Joplin, Missouri	*PAR	Parsons, Kansas	SUJ	Sioux Falls, South Dakota
KFR	Kingsfisher, Oklahoma	PHP	Philip, South Dakota	SUX	Sioux City, Iowa
LAF	Lafayette, Indiana	PIA	Peoria, Illinois	TOP	Topeka, Kansas
LBB	Lubbock, Texas	PIR	Pierre, South Dakota	*TRO	Toronto, Kansas
LBF	North Platte, Nebraska	PUB	Pueblo, Colorado	TUL	Tulsa, Oklahoma
LHX	La Junta, Colorado	PNC	Ponca City, Oklahoma	TXK	Texarkana, Arkansas
LIT	Little Rock, Arkansas	*PSK	Pawhuska, Oklahoma	UIN	Quincy, Illinois
LMN	Lamoni, Iowa	*PWN	Pawnee, Oklahoma	VIH	Vichy, Missouri
LNK	Lincoln, Nebraska	RAN	Rantoul, Illinois	VLA	Vandalia, Illinois

(b) Words in Figures

BLGS	buildings	GRD	ground	SFTED	shifted
CLD(S)	cloud(s)	INJRD	injured	SWIG	swelling
COND	condensation	OCF	occluded front	TCHED	touched
CY	cyclone	QUDS	quadrants	TORDO	tornado
DEMSHED	demolished	RCHING	reaching	TSTM	thunderstorm
DIA	diameter	REP	report	TWRG	thundering
DMGE(D)	damage(d)	RW(U)	rainshower (unknown)	UPD	updraft
DWD	downdraft	SCT	scattered		
FUNL	funnel	SFC	surface		

* Accelerated Barograph Station.

REFERENCES

- BERGERON, T., 1954: Tropical hurricanes, *Quart. J. Roy Met. Soc.*, No. 344, pp. 131—164.
- BJERKNES, J. and SOLBERG, H., 1923: Meteorological conditions for the formation of rain, *Geophysiske Publikationer, II*, pp. 4—60.
- BROOKER, C. F., 1922: The local, or heat, thunderstorm, *Mo. Wea. Rev.*, U.S. Weather Bureau No. 50, pp. 281—287.
- BROOKS, E. M., 1949: The tornado cyclone, *Weatherwise*, 2, 2, pp. 32—33.
- BROOKS, E. M., 1954: Characteristics of thunderstorm microbarographs, *Trans. Amer. Geoph. Union*, 35, 3, pp. 413—419.
- BYERS, H. R., 1942: Nonfrontal thunderstorms, *Dep. Meteor. Univ. Chicago, Misc. Rep.*, No. 3.
- BYERS, H. R. and HULL, E. C., 1949: Inflow patterns of thunderstorms as shown by wind aloft, *Bull. Am. Met. Soc.*, 30, 3, pp. 90—96.
- BYERS, H. R. and BRAHAM, R. R. JR., 1949: *The Thunderstorm*, Report of the Thunderstorm Project, 1946 and 1947, Government Printing Office, Washington, D.C.
- Climatological Data, *National Summary*, 4, 6, 1953, p. 181.
- FUJITA, T., 1950: Microanalytical study of thundernose, *Geoph. Mag. of Japan*, 22, 2, pp. 71—88.
- FUJITA, T., 1951: Microanalytical study of cold front, *Geoph. Mag. of Japan*, 22, 2, pp. 237—277.
- FULKS, J. R.: On the mechanics of the tornado (unpublished).
- PENN, S., PIERCE, C., and MCGUIRE, J. K., 1955: The squall line and Massachusetts tornadoes of June 9, 1953, *Bull. Am. Met. Soc.*, 36, 3, pp. 109—122.
- SUCKSTORFF, G. A., 1953: Die Strömungsvorgänge in Instabilitätsschauern, *Meteor. Zeitschrift*, 52, Heft 12, pp. 449—452.
- SWINGLE, D. M. and ROSENBERG, L., 1953: Mesometeorological analysis of cold front passage using radar weather data, *Proc. Conf. on Radar Meteor.*, Univ. of Texas, Ch. XI-5.
- TEPPER, M., 1950: A proposed mechanism of squall-line: the pressure jump, *J. Met.*, 7, pp. 21—29.
- WILLIAMS, D. T., 1948: Surface micro study of squall-line thunderstorms, *Mo. Wea. Rev.*, 76, 11, pp. 239—246.